Titre: Title:	Oxygen Diffusion and Consumption in Unsaturated Cover Materials
Auteurs: Authors:	M. Mbonimpa, M. Aubertin, M. AAchib and B. Buissière
Date:	2002
Type:	Rapport / Report
Référence: Citation:	Mbonimpa, M., Aubertin, M., Buissière, B. et AAchid, M. (2002). Oxygen Diffusion and Consumption in Unsaturated Cover Materials. Rapport technique. EPM-RT-2002-04.

EPM–RT–2002-04

OXYGEN DIFFUSION AND CONSUMPTION IN UNSATURATED COVER MATERIALS

M. Mbonimpa, M. Aubertin, M. AAchib, and B. Buissière
Département des génies civil, géologique et des mines
École Polytechnique de Montréal

Décembre 2002

EPM-RT-2002-04

OXYGEN DIFFUSION AND CONSUMPTION IN UNSATURATED COVER MATERIALS

M. MBONIMPA[A,1], M. AUBERTIN[A,1], M. AACHIB[B], and B. BUSSIÈRE[C,1]

[A] Department of Civil, Geological and Mining Engineering, École Polytechnique de Montréal, P.O. Box 6079, Stn. Centre-ville, Montreal, Québec, H3C 3A7, Canada.

[B] Department of Hydraulic, École Hassania des Travaux Publics, km 7, Route El Jadida, B.P. 8108, Casablanca-Oasis, Maroc.

[C] Department of Applied Sciences, Université du Québec en Abitibi-Témiscamingue (UQAT), 445 boul. de l'Université, Rouyn-Noranda, Québec, J9X 5E4 Canada.

[1] Industrial NSERC Polytechnique-UQAT Chair on Environment and Mine Wastes Management

DECEMBER 2002

Dépôt légal :
Bibliothèque nationale du Québec, 2002
Bibliothèque nationale du Canada, 2002

EPM-RT-2002-04
Oxygen diffusion and consumption in unsaturated cover materials
by: Mamert Mbonimpa[A,1], Michel Aubertin[A,1*], Mostafa Aachib[B], et Bruno Bussière[C,1]

[A] Department of Civil, Geological and Mining Engineering, École Polytechnique de Montréal
[B] Dep. of Hydraulic, École Hassania des Travaux Publics, Casablanca-Oasis, Maroc
[C] Department of Applied Sciences (UQAT), Rouyn-Noranda
[1] Industrial NSERC Polytechnique-UQAT Chair on Environment and Mine Wastes Management

ABSTRACT

In many environmental geotechnique problems, engineers must analyse situations where water and gas can move simultaneously. Such is typically the case when soil covers are designed for waste disposal sites. Being located well above the phreatic surface, cover materials are unsaturated and may allow gaseous compounds (such as air and methane) to flow in or out from the disposal facilities. As is the case for water, the flow of gas must usually be controlled by the cover. A particular application in that regard relates to covers built to limit oxygen flux to reactive sulphidic tailings, which can be the source of an acidic leachate. In this paper, the authors present an approach to evaluate the oxygen flux with the controlling parameters, including the effective diffusion coefficient D_e and the reaction (consumption) rate coefficient K_r. An experimental procedure to determine these two parameters simultaneously during laboratory experiments is described, and sample results are presented with the proposed interpretation. Analytical solutions are further developed to calculate oxygen flux through cover materials. The proposed solutions are compared to calculation results ensuing from a numerical treatment of modified Fick's laws. A variety of specific applications of the method for designing oxygen barriers are also presented and discussed.

Keywords: unsaturated soil covers, Fick's laws, oxygen diffusion, acid mine drainage, analytical solutions, numerical solutions.

RÉSUMÉ

Dans plusieurs problèmes de géotechnique environnementale, les ingénieurs doivent analyser des situations d'écoulement simultané d'eau et de gaz. C'est typiquement le cas lorsque des couvertures en sol sont conçues pour des sites d'entreposage de rejets. Étant placés bien au-dessus de la surface phréatique, les matériaux de recouvrement sont non saturés, et ils peuvent permettre à des composés gazeux (tels que l'air et le méthane) d'entrer ou de s'échapper du site. Comme c'est le cas avec l'eau, le flux de gaz doit habituellement être contrôlé par le recouvrement. Une application particulière à cet égard concerne les couvertures construites pour limiter le flux d'oxygène vers les résidus miniers sulfureux, qui peuvent générer un lixiviat acide. Dans cet article, les auteurs présentent une approche pour évaluer ce flux et les paramètres de contrôle, incluant le coefficient de diffusion effectif D_e et le coefficient du taux de réaction (ou de consommation) K_r. Un procédé expérimental pour la mesure simultanée de ces deux paramètres en laboratoire est décrit, et une procédure d'interprétation avec quelques résultats d'essais sont présentés. Des solutions analytiques sont de plus développées pour calculer le flux d'oxygène à travers des systèmes de recouvrement. Ces solutions sont comparées aux résultats obtenus d'un traitement numérique des lois de Fick modifiées. Diverses applications spécifiques de la méthode de conception des barrières à l'oxygène sont présentées et discutées.

Mots clés : couvertures en sol non saturé, lois de Fick, diffusion de l'oxygène, drainage minier acide, solutions analytiques, solutions numériques.

ACKNOWLEDGEMENTS

The post-doctoral grant provided to the first author (Mamert Mbonimpa) by the Institut de Recherche en Santé et Sécurité du Travail du Québec (IRSST) is thankfully acknowledged. Special thanks also go to Antonio Gatien and to the graduate students who performed the diffusion tests over the years. The authors also received financial support from NSERC and from a number of industrial participants to the industrial NSERC Polytechnique-UQAT Chair on Environment and Mine Wastes Management.

TABLE OF CONTENTS

LIST OF NOTATIONS

b	proportionality factor between $L_{T,R}$ and D_e (see Figure 19) (-)
$C(z, t)$	interstitial oxygen concentration in the gas phase at time t and position z (%, or mole/m^3, or kg/m^3)
C_0	oxygen concentration at the upper surface (z=0) (%, or mole/m^3, or kg/m^3)
$C_1(z, t)$	oxygen concentration in the gas phase at time t and position z; particular form used in eq. 12 (%, or mole/m^3, or kg/m^3)
C_a	equilibrium concentration of oxygen in air (%, or mole/m^3, or kg/m^3)
C_L	oxygen concentration at depth z=L (%, or mole/m^3, or kg/m^3)
C_p	pyrite content over mass of dry tailings (kg/kg). (eq. 25)
C_U	uniformity coefficient ($C_U = D_{60}/D_{10}$) [-]
C_w	maximum concentration (solubility) of oxygen in water (%, or mole/m^3, or kg/m^3)
D_{10}	diameter corresponding to 10 % passing on the cumulative grain-size distribution curve [L]
D_{60}	diameter corresponding to 60 % passing on the cumulative grain-size distribution curve [L]
D^0	free diffusion coefficient in a free (non obstructed) medium [L^2T^{-1}]
D_a^0	free oxygen diffusion coefficient in air (eq. 19) [L^2T^{-1}]
D_w^0	free oxygen diffusion coefficient in water (eq. 19) [L^2T^{-1}]
D_a	diffusion coefficient component in the air phase (eq. 18) [L^2T^{-1}]
D_e	effective diffusion coefficient [L^2T^{-1}]
$D_{e,j}$	effective diffusion coefficient of layer j (eq. 34) [L^2T^{-1}],
D_H	equivalent grain size diameter D_H (eqs 25 and 26) [L]
D_j*	bulk diffusion coefficient of layer j (eq. 34) [L^2T^{-1}]
D_w	diffusion coefficient in the water phase (eq. 18) [L^2T^{-1}]
$\overline{D}_e$	mean effective equivalent diffusion coefficients (eq. 33) [L^2T^{-1}]
$\overline{D}^*$	mean bulk equivalent diffusion coefficients (eq. 34) [L^2T^{-1}]

E	efficiency factor (eq. 28) (%)
$F(z,t)$	diffusive flux of O_2 at position z and time t [$ML^{-2}T^{-1}$]
F_0	oxygen flux at the surface of the uncovered tailings (eq.)[$ML^{-2}T^{-1}$]
$F_{0,s}$	surface flux under steady state conditions (eqs. 30 and 31) [$ML^{-2}T^{-1}$]
$F_1(z,t)$	flux obtained for non reactive cover material; form used in eq. 13 [$ML^{-2}T^{-1}$]
f_p	proportionality factor between t_{ss} and L^2/D^* (eq. 11) (-)
$F_{s,L}$	flux at the base of the layer under steady state conditions (eq. 10) [$ML^{-2}T^{-1}$]
H	dimensionless Henry's equilibrium constant given by the ratio $H=C_w/C_a$
K_r	oxygen reaction (consumption) rate coefficient [T^{-1}].
K_r^*	bulk reaction rate coefficient [T^{-1}]
K'	intrinsic reactivity of pyrite with oxygen (eq. 25) (m^3 O_2/m^2pyrite/s)
L	thickness [L]
L_j	thickness of layer j (eqs. 33 to 35) [L]
L_T	homogeneous layer thickness representing the reactive tailings [L]
$L_{T,R}$	reference thickness above which the flux becomes independent of the tailings thickness L_T (eq.s. 32) [L]
m	number of layers (eqs. 33 to 35)
n	porosity (-)
$Q(z=L,T)$	total amount of the substance diffusing through the cover at a given depth $z=L$ and time t [ML^{-2}]
Q_0	incoming global flux at the surface of the uncovered reactive tailings (eq. 29 [ML^{-2}]
Q_{ss}	total amount of the substance diffusing through the cover under steady state conditions [ML^{-2}].
S_r	degree of saturation (-)
t	time [T]
$t^*_{1/2}$	half-time life used to define the reaction rate coefficient in the case of a first-order kinetic (eq. 27) [T]
T_a	tortuosity coefficients for the air phase (eqs. 19 and 20)
t_a	active period in which diffusion and consumption occurs in a cover

t_{ss} time necessary to reach the steady state (eq. 11) [T]

T_w tortuosity coefficients for the water phase (eqs. 19 and 21)

$t_{ss\text{-}90}$, $t_{ss\text{-}95}$, $t_{ss\text{-}99}$, $t_{ss\text{-}99.99}$ time necessary to reach 90, 95, 99, and 99.99 % of the steady state flux at the base of a cover[T]

$t_{ss\text{-}100.01}$ time necessary to reach 100.01 % of the steady state flux at the surface of a cover [T]

x, y material parameter (eqs. 22 and 23) (-)

z position (depth) [L]

$\theta_{eq,j}$ equivalent porosity of layer j (eq. 35) (-)

θ_a air filled porosity (-)

θ_{eq} equivalent diffusion porosity (eq. 3) (-)

$\overline{\theta}_{eq}$ mean equivalent porosity (eq. 35) (-)

θ_w volumetric water content (-)

LIST OF FIGURES

LIST OF TABLES

1. INTRODUCTION

Quantifying fluid flow in soils above the water table, in the vadose zone where unsaturated conditions prevail, is a challenging problem that bears significance to many areas of human activities, including civil engineering, agriculture and forestry. In these various fields, engineers and scientists have worked at developing models for predicting how liquids and gases move according to acting driving forces, generally emphasizing the effect of pressure and concentration gradients. Examples of such type of applications include: aeration in cultivated soils; exchanges around roots in relation to bacterial activity, denitrification, and degradation of organic matter; treatment of contaminated soils by venting techniques.

In geotechnical engineering, a lot of attention has been paid over the last two decades or so, to the proper analysis and design of surface disposal sites for various types of wastes (industrial, domestic, etc.). To control the exchanges between the wastes and the surrounding environment, the surface is often covered upon closure by an hydrogeological barrier known as a cover or cap. Today, layered covers, made of different types of materials, are commonly used to control infiltration of water and also to limit gas flux (methane, carbon dioxide, oxygen, radon, etc.) in and out from the waste disposal sites.

Multilayered cover systems are also increasingly popular in the mining industry as an effective means of reducing the production of acid mine drainage (AMD) ensuing from the oxidation of sulphidic minerals in rock wastes and mill tailings (e.g. SRK 1989; Collin and Rasmuson 1990; Yanful 1993; MEND 2001). The processes involved in the generation of AMD from sulphide rich minerals have been intensively investigated over the years (e.g. Jambor and Blowes 1994). These studies have shown that preventing oxygen from reaching the reactive materials constitutes a practical approach for controlling the production of acidic leachate.

In that regard, there is one particular type of layered cover that has been used with success on a few sites in Canada in recent years, i.e. covers with capillary barrier effects or CCBE (e.g. Woyshner and Yanful 1995; Ricard et al. 1997, 1999; Wilson et al. 1997; Aubertin et al. 1997a, 1999; O'Kane et al. 1998; Dagenais et al. 2001). An idealised section of a CCBE, comprising up to five layers, is shown in Figure 1.

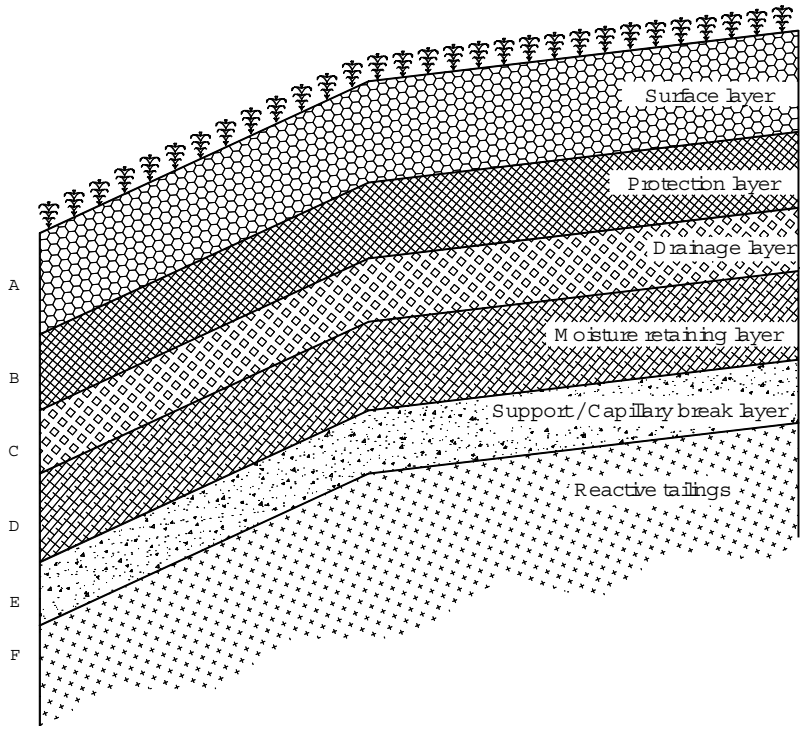

Figure 1. Typical section of a multi-layered cover with capillary barrier effects (after Aubertin et Chapuis 1991; Aubertin et al. 1995).

The specific role and nature of the different layers and materials have been described in details in Aubertin et al. (1993, 1995) and in the other references on CCBE mentioned above. In such a CCBE, the differing hydrogeological properties of the various soils (and other particulate media) are used to enhance water retention in one of the layers (i.e. the moisture retaining layer in Figure 1). In a relatively arid area, CCBE can be employed to reduce vertical percolation of water into the wastes by storage, lateral drainage, and evaporation (e.g. Zhan et al. 2001). In a rather humid area, CCBE are mainly used to impede the passage of oxygen from the atmosphere to the reactive

materials underneath (e.g. Nicholson et al. 1989; Collin and Rasmuson, 1990; Aubertin and Chapuis, 1991; Aachib et al. 1993).

To establish the design basis of a CCBE, one must analyse the flow of water in the layered system located above the water table. Unsaturated water flow and humidity distribution in CCBE have been studied by a number of groups, and the corresponding behavior is now fairly well understood (e.g. Akindunni et al. 1991; Aubertin et al. 1995, 1996, 1997b; Aachib 1997; Bussière et al. 2000).

For CCBE used as an oxygen barrier, attention must also be paid to evaluating the gas flux. In this case, the efficiency of the cover system is related to the reduced capacity of air (oxygen) to move through a highly saturated medium, whether it is by advection or by diffusion. This reduced mobility is used to diminish the oxygen flux, and hence to control production of AMD (Collin and Rasmuson 1988; Nicholson et al. 1989; Aachib et al. 1993).

To determine the final (optimal) configuration of a cover, one needs to evaluate the anticipated flux based on the moisture distribution in the layers. Because molecular diffusion is generally the controlling mechanism, this in turn requires that the effective diffusion coefficient D_e be evaluated, either from in situ measurements (e.g. Rolston et al. 1991; Mbonimpa et al. 2000) or, more commonly, from laboratory tests (e.g. Reardon and Moodle 1985; Yanful 1993; Aubertin et al. 1995, 1999, 2000b; Shelp and Yanful 2000).

In some cases, the oxygen flux through a cover may be influenced by the reactivity of a material used in one of its layers (Aubertin et al. 2000a). This is the case for instance when organic matter is used in the cover (e.g. Cabral et al. 2000), or when a small amount of iron sulphides (like pyrite and pyrrhotite) is present in the cover material (Mbonimpa et al. 2000). Having oxygen being consumed in a low flux cover can often be advantageous, as it may help reduce the amount of O_2 that reaches the reactive wastes underneath. In this situation, the measurement technique and the flux calculation procedure must take both phenomena (diffusion and consumption) into account.

In the following, the authors use modified Fick's laws to describe oxygen transport mechanisms in unsaturated porous materials. Analytical solutions are developed to estimate the oxygen flux that reaches reactive tailings (or rock wastes) under a cover, for boundary and initial conditions similar to those that prevail in actual CCBE, for cases of non reactive as well as reactive (but non acid generating) cover materials. A procedure to measure the controlling oxygen transport parameters, i.e. the diffusion coefficient D_e and the reaction (consumption) rate coefficient K_r, is also described. Measurements data are interpreted using the software POLLUTE v6 (Rowe et al. 1994), which provides numerical solutions to Fick's laws. This software is also employed to validate the proposed analytical solutions. Significant issues for various practical applications, including the influence of the key properties on the oxygen flux, are treated with sample calculations.

2. OXYGEN TRANSPORT IN COVERS

In a partly saturated media with small pore size, such as fine grained soils used in covers (i.e. silts and clays), oxygen transport is generally controlled by molecular diffusion (Collin 1987; Collin and Rasmuson 1988). Such diffusion through the voids mostly occurs in the air phase, at least when the degree of saturation S_r is below about 85 to 90%. Above such S_r value however, the air phase, characterised here by the air filled porosity θ_a $(=n(1-S_r)$ where n is porosity), becomes discontinuous (Corey 1957). The diffusion flux then also involves transport through the water filled voids, characterised here by the volumetric water content θ_w $(= n\ S_r = n-\theta_a)$. In this latter case, the amount of oxygen that can flow is limited by the maximum concentration (solubility) of O_2 in water (C_w), which is about than 30 times less than the equilibrium concentration of oxygen in air (C_a) (≈ 276.7 mg/l) at 20°C.

Fick's laws are commonly used to evaluate diffusion transport for elements in a soluble state (e.g. Freeze and Cherry 1979; Shackelford 1991), as well as in a gaseous phase (Troeh et al. 1982, Reible and Shair 1982; Reardon and Moddle 1985; Jin and Jury 1996; Aachib 1997). In the corresponding equations presented below, concentration variation over time and space is related to the effective diffusion coefficient of the material D_e, which in turn depends on the pore size (or

relative volume of voids) and tortuosity, and also on the diffusion coefficient of the element in a free (non obstructed) medium. Because the latter coefficient is about 10000 times larger in air than in water, transport or oxygen in the water filled pores is much slower than in the air filled voids. When adding the relatively small equilibrium concentration of O_2 in water to such reduced diffusion coefficient in the free phase, it becomes easy to understand why a CCBE having a highly saturated layer can be efficient in controlling oxygen flux. In this case, the layer that remains close to saturation impedes the passage of O_2, hence reducing the generation of acid mine drainage due to oxidation of sulphidic minerals (Collin 1987; Nicholson et al. 1989).

When a material layer through which it flows reacts with oxygen, the overall flux that completely go across the cover can be decreased significantly. To evaluate the magnitude of this effect, the amount of oxygen that is "consumed" by the reactive material in the cover must be determined. This amount depends on a reaction (consumption) rate coefficient K_r, which varies with the reactivity of the minerals, the grains specific surface area, and the porosity of the media.

So far, relatively few studies have been conducted on the combined use of (modified) Fick's laws, with D_e and K_r, to establish the efficiency of AMD control measures. Elberling and coworkers have used laboratory and in situ tests for identifying these parameters using oxygen consumption tests (e.g. Elberling et al. 1994; Elberling and Nicholson 1996). This technique, with an interpretation that relies on a pseudo-steady state condition for a semi-infinite reactive media, is not directly applicable to the situation described here. Cabral et al. (2000) have made some interesting measurements on organic materials to establish the value of D_e and K_r, and the corresponding flux through a cover. However, this technique was developed mainly for highly reactive cover materials, and some limitations to their approach have been identified and discussed elsewhere (Aubertin and Mbonimpa 2001).

A somewhat different approach is proposed here to evaluate simultaneously the required parameters (D_e and K_r) through a simple procedure with a novel interpretation of laboratory tests results. The proposed solution relies on a general numerical solution of modified Fick's laws, as provided by the POLLUTE software (developed by Rowe et al. 1994). These parameters are used with new analytical solutions to evaluate the flux through cover systems.

2.1 Basic equations

The oxygen flux *F(z, t)* and concentration *C(z, t)* at position *z* and time *t* are determined from the first and second Fick's laws, given for one-dimensional diffusion as (Hillel 1980):

$$[1] \qquad F(z,t) = -D_e \frac{\partial C(z,t)}{\partial z}$$

$$[2] \qquad \frac{\partial}{\partial t}(\theta_{eq} C) = \frac{\partial}{\partial z}(D_e \frac{\partial C}{\partial z})$$

In these equations *F(z,t)* is the diffusive flux of O_2 [$ML^{-2}T^{-1}$], D_e is the effective diffusion coefficient [L^2T^{-1}], *C(z, t)* is the interstitial O_2 concentration at time *t* [T] and position *z* [L], and θ_{eq} is an equivalent (diffusion) porosity [L^3L^{-3}]; θ_{eq} is used here instead of θ_a which has been often used in the past (Yanful 1993; Aubertin et al. 1995). The need to use θ_{eq} to evaluate the oxygen flux through covers with Fick's laws can be deduced from the work of Collin (1987) (see also Collin and Rasmuson 1988). The equivalent porosity θ_{eq} is employed here to take into account the flux in the air phase and the flux of oxygen dissolved in the water phase. It is defined as (Aubertin et al. 1999, 2000b):

$$[3] \qquad \theta_{eq} = \theta_a + H\theta_w$$

where *H* is the dimensionless Henry's equilibrium constant given by the ratio $H=C_w/C_a$. For oxygen, $H \cong 0.03$ at 20°C.

Equation 2 is only valid for diffusion through an inert material where no O_2 generation or consumption occurs. This second Fick's law can be modified to consider the effect of varying concentration of the moving substance due to reaction with the medium (Crank 1975; Schackelford 1991). If the diffusing gas is "immobilized" by an irreversible first-order kinetic

reaction (or exponential decay), as is usually assumed for sulphidic mineral reactions (e.g. Elberling and Nicholson 1996; Yanful at al. 1999), this law can be modified as follows:

$$[4] \qquad \frac{\partial}{\partial t}(\theta_{eq} C) = \frac{\partial}{\partial z}(D_e \frac{\partial C}{\partial z}) - K_r C$$

where K_r is the reaction rate coefficient [T^{-1}].

To enhance the generality of the solutions, D_e and K_r will be expressed respectively as functions of the bulk diffusion coefficient D^* [L^2T^{-1}] and bulk reaction rate coefficient K_r^* [T^{-1}]:

$$[5] \qquad D_e = \theta_{eq} D^*$$

and

$$[6] \qquad K_r = \theta_{eq} K_r^*$$

In the following, θ_{eq} and D_e will be taken as independent of time t and depth z in a given material layer; this is a simplifying assumption that is not required for a full theoretical development but which facilitates the demonstration and calculations. In this case, equations 4 can be rewritten as:

$$[7] \qquad \frac{\partial C}{\partial t} = D^* \frac{\partial^2 C}{\partial z^2} - K_r^* C$$

Even with these simplifications, solving equations 1 and 7 for relatively complex boundary conditions often requires a numerical treatment. Such is usually considered to be the case for multilayered structures like covers. Differential equation 7 can also be solved analytically under well defined, but relatively simple boundary conditions for steady as well as transient state conditions, to obtain the concentration profile *C(z,t)* (Barrer 1941; Jost 1952; Carslaw and Jaeger1959; Astarica 1967; Crank 1975), which in turn can provide the flux (with eq. 1). Some

typical solutions are presented in the following for the case of diffusion through an homogeneous layer with a thickness L, satisfying the boundary conditions $C(z=0,\ t>0) = C_0$ (the concentration at the upper interface is constant; $C_0 \equiv C_a$) and $C\ (z \geq L,\ t>0) = C_L = 0$ (the concentration at the lower interface is zero), with the initial condition $C(z>0,\ t=0) = 0$ (the initial concentration throughout the medium pores is zero).

2.2 Equations for O_2 flux

For a non reactive material layer with a bulk diffusion coefficient D^*, the concentration function $C(z,t)$ can be obtained from equation 7 with $K_r = 0$ using the method of variables separation (Adda and Philbert 1966; Crank 1975). The solution obtained with this method is written in the form of a trigonometrical series:

$$[8] \qquad C(z,t) = C_0\left[1 - \frac{z}{L} - \frac{2}{\pi}\sum_{i=1}^{\infty}\frac{1}{i}\sin\frac{i\pi z}{L}\exp\left(-\frac{i^2\pi^2}{L^2}D^*t\right)\right]$$

where i is an integer. The authors have used this solution with equation 1 to obtain the flux $F(z=L,\ t>0)$ at the base of the layer ($z=L$; $C_L=0$). The ensuing equation can be written as:

$$[9] \qquad F(z=L,\ t>0) = F_{s,L} + 2F_{s,L}\sum_{i=1}^{\infty}(-1)^i\exp\left(-\frac{i^2\pi^2}{L^2}D^*t\right)$$

where $F_{s,L}$ is the oxygen flux at the base of the layer under steady state conditions. When considering a rapid and complete consumption of O_2 below the cover (C_L=0), this flux is expressed as:

$$[10] \qquad F_{s,L} = \frac{C_0 D_e}{L}$$

The time necessary to reach steady state can also be estimated semi-analytically (Crank 1975). The proposed solution for that purpose is:

$$[11] \qquad t_{s,L} \approx \frac{f_p L^2}{D^*}$$

where f_p is a proportionality factor; a value f_p=0.45 was suggested by Crank (1975) for general applications (this value will be revisited below).

For a reactive cover material with a bulk diffusion coefficient D^* and a bulk reaction rate coefficient K_r^*, the flux at the base of the layer ($z=L$) can be derived using the Danckwert's method (Crank 1975). According to this method, if $C_1(z,t)$ (given by eq. 8) is a solution to equation 7 with K_r = 0, the general solution (for $K_r \geq 0$) of equation 7 for the same boundary conditions takes the following form:

$$[12] \qquad C(z,t) = K_r^* \int_0^t C_1(z,t') \exp(-K_r^* t') dt' + C_1(z,t) \exp(-K_r^* t)$$

This equation is introduced into equation 1 to evaluate the flux, which becomes:

$$[13] \qquad F(z,t) = K_r^* \int_0^t F_1(z,t') \exp(-K_r^* t') dt' + F_1(z,t) \exp(-K_r^* t)$$

in which $F_1(z,t)$ is the flux obtained for a non reactive material using the solution for $C_1(z,t)$ (equation 8). For $z=L$ (below the cover layer), F_1 is given by equation 9. Introducing this expression into equation 13 and integrating leads to the following expression for the flux below the cover (at $z=L$):

$$F(z=L,\,t>0)=F_{s,L}+2K_r^{*}F_{s,L}\sum_{i=1}^{\infty}\frac{(-1)^i}{\frac{i^2\pi^2D^{*}}{L^2}+K_r^{*}}+$$

[14]
$$2F_{s,L}\sum_{i=1}^{\infty}(-1)^i\,exp\left(-(\frac{i^2\pi^2D^{*}}{L^2}+K_r^{*})t\right)-$$

$$2K_r^{*}F_{s,L}\sum_{i=1}^{\infty}\frac{(-1)^i}{\frac{i^2\pi^2D^{*}}{L^2}+K_r^{*}}exp\left(-(\frac{i^2\pi^2D^{*}}{L^2}+K_r^{*})t\right)$$

Again, $F_{s,L}$ is given by equation 10. After a sufficiently long time of oxygen diffusion under constant boundary conditions, a steady state may be attained. The corresponding flux F_{ss} reaching the reactive materials below the cover is then given by :

[15]
$$F_{ss}(z=L,\,t\to\infty)=F_{s,L}+2K_r^{*}F_{s,L}\sum_{i=1}^{\infty}\frac{(-1)^i}{\frac{i^2\pi^2D^{*}}{L^2}+K_r^{*}}$$

It is interesting to note that equations 9 and 10 (for $K_r^{*} = 0$) are particular cases of the more general expressions (eq. 14 and 15) developed for $K_r^{*} \geq 0$. The proposed analytical solutions will be validated below through comparisons with numerical solutions, and will then be used to evaluate the oxygen flux through cover systems (see section 4).

Equations 14 and 15 give the flux reaching the bottom of the cover. It can also be useful in some cases to evaluate the flux F entering the cover (for z=0). The expression to calculate this flux can be obtained in the same manner as equation 14. The following equation is then obtained:

$$F(z=0,\,t>0) = F_{s,L} + 2K_r{}^{*} F_{s,L} \sum_{i=1}^{\infty} \frac{1}{\frac{i^2\pi^2 D^{*}}{L^2} + K_r{}^{*}} +$$

[16]
$$2F_{s,L} \sum_{i=1}^{\infty} exp\left(-\left(\frac{i^2\pi^2 D^{*}}{L^2} + K_r{}^{*}\right)t\right) -$$

$$2K_r{}^{*} F_{s,L} \sum_{i=1}^{\infty} \frac{1}{\frac{i^2\pi^2 D^{*}}{L^2} + K_r{}^{*}} exp\left(-\left(\frac{i^2\pi^2 D^{*}}{L^2} + K_r{}^{*}\right)t\right)$$

From equation 16, the steady state flux can equally be estimated as follows:

[17]
$$F_{ss}(z=0,\,t\to\infty) = F_{s,L} + 2K_r{}^{*} F_{s,L} \sum_{i=1}^{\infty} \frac{1}{\frac{i^2\pi^2 D^{*}}{L^2} + K_r{}^{*}}$$

In the case of reactive materials (K_r>0), the steady state fluxes entering and leaving the cover are different (compare eqs. 15 and 17), due to oxygen consumption. For non reactive materials (K_r=0), these fluxes are similar.

To apply these solutions, the diffusion coefficient D^{*} and the reaction rate coefficient $K_r{}^{*}$ (and thus D_e et K_r) have to be determined. The laboratory testing procedure and the interpretation method developed to this end are shown below. Validation and applications of the proposed equations are presented afterwards.

3. PARAMETER DETERMINATION

3.1 Testing procedure

Various experimental approaches have been used to determine the effective diffusion coefficient D_e of inert (non reactive) materials (e.g. Reible and Shair 1982; Shakelford 1991; Tremblay 1995; Mackay et al. 1998). The authors present here a procedure that evolved from the approach described previously in Aubertin et al. (1995, 1999, 2000a, 2000b). It allows a simultaneous evaluation of D^* and K_r^* (or D_e and K_r) for reactive materials. The measurements are performed with the diffusion cell shown in Figure 2.

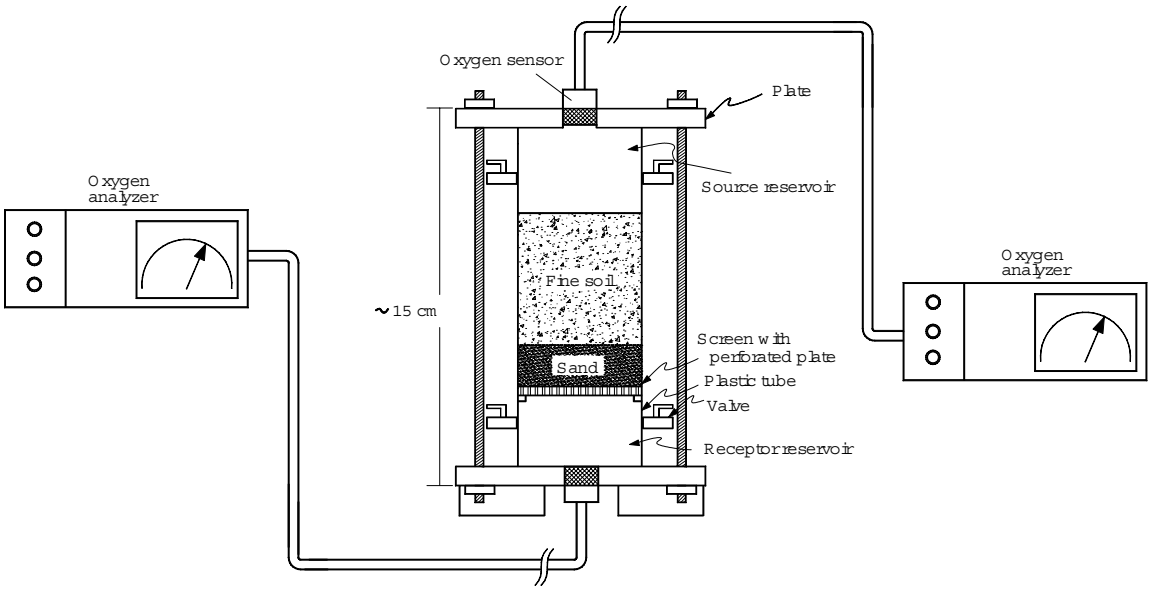

Figure 2. Schematic representation of a diffusion cell used to evaluate oxygen flux parameters; the concentration measurement in both reservoirs allows a simultaneous determination of the effective diffusion coefficient D_e and of the reaction rate coefficient K_r (adapted from Aubertin et al. 1995, 1999).

The testing procedure can be summarized as follows. The material layer (about 5 cm thick) is first brought to the desired degree of saturation and density (porosity) into the cell. The water content in the tested material can be brought up to (almost) full saturation by the capillary barrier

effect created by the underlying coarse grained material (a concrete sand is typically used with a silty reactive material). This coarse material layer (about 3 cm thick) drains and remains fairly dry, thus having little influence on oxygen flux. The negligible differences obtained between the water contents measured before and after the tests have confirmed the efficiency of this practice to control moisture in fine grained materials.

At the beginning of the test, the entire cell is purged with humidified nitrogen until the oxygen concentration of the entire cell stabilizes to zero (almost no entrapped oxygen remains in the sample). The source reservoir is then briefly opened to reach atmospheric conditions (oxygen concentration C_0 of about 20.9%, or 9.3 mole/m^3, or 276 mg/l). Once the cell is closed, oxygen migrates by diffusion from the source to the receptor reservoir (initially void of O_2) due to the concentration gradient. The temporal evolution of oxygen concentration in the two reservoirs is measured with oxygen sensors (Teledyne type were used) fixed to the reservoirs plates, each of which is connected to an oxygen analyser (calibrated before each use). One can use the measured concentration evolution in each reservoir, and the ensuing mass balance, to determine D^* and K_r^* (or D_e and K_r).

For these testing conditions, solutions provided by POLLUTE (or by numerical solutions programmed on Matlab - e.g. Aachib and Aubertin 2000) allow a calculation of the oxygen concentration in the two reservoirs for given values of D^* and K_r^*. The actual parameter values of the tested material are obtained iteratively by comparing the measured and calculated concentration profiles. The selection of the D^* and K_r^* values that allow a "best fit" to the experimental data follows a sensitivity analyses. For this curve fit procedure, the initial values of D^* and K_r^* are obtained from equations 5 and 6, using D_e and K_r values estimated from the semi-empirical expressions presented below. More information on the experimental and determination procedure was presented by Aachib and Aubertin (2000).

3.2 Semi-empirical estimates

Measurement of the effective diffusion and reaction rate coefficients is required to adequately evaluate the flux for optimum cover design. Nevertheless, it is often very useful to have an approximate value of these parameters beforehand, to establish some basic design conditions at the preliminary phase of a project, to initiate the determination procedure described above, or to validate some questionable experimental results. For that purpose, semi-empirical expressions have been proposed to estimate these parameters from basic material properties, such as porosity and degree of saturation (e.g. Marshall 1959; Reardon and Moddle 1985; Elberling et al. 1994). More information on this aspect can be found in Aachib et al. (2002).

For D_e, the expression used here follows the concept developed by Millington and Quirk (1961) and Millington and Shearer (1971), and later modified by Collin (1987). This approach has been successfully applied by the authors to a variety of test results (Aubertin et al. 1995, 1999, 2000a, 2000b). The effective diffusion coefficient can be expressed as:

[18] $$D_e = D_a + HD_w$$

with

[19] $$D_a = \theta_a D_a^0 T_a \qquad \text{and} \qquad D_w = \theta_w D_w^0 T_w \ .$$

In these equations, D_a and D_w are the diffusion coefficient components in the air phase and water phase respectively. D_a^0 and D_w^0 are the free oxygen diffusion coefficient in air and in water respectively; at room temperature $D_a^0 \cong 1.8\text{x}10^{-5}$ m^2/s and $D_w^0 \cong 2.5\text{x}10^{-9}$ m^2/s (Scharer et al. 1993). Parameters T_a and T_w are the tortuosity coefficients for the air and water phases. These coefficients can be related to basic properties using the Collin (1987) model (see also Collin and Rasmuson 1988). One can then write:

[20] $$T_a = \frac{\theta_a^{2x+1}}{n^2}$$

and

[21] $$T_w = \frac{\theta_w^{2y+1}}{n^2}$$

The value of x and y can be obtained from the following conditions:

[22] $$\theta_a^{2x} + (1-\theta_a)^x = 1$$

[23] $$\theta_w^{2y} + (1-\theta_w)^y = 1$$

For instance, these relationships mean that for n=0,4, y varies approximately from 0.54 to 0.68 and x from 0.68 to 0.54 when the material goes from a dry state to a saturated state. Alternatively, a fixed value of 0.65 has been adopted by Aachib et al. (2002) for both x and y in eqs. 20 and 21, as this provides the most realistic estimate of the tortuosity factor for fully dry (S_r=0) and fully saturated (S_r=1) conditions, according to the experimental results analysed. The following expression was then proposed (Aachib and Aubertin 2000):

[24] $$D_e = \frac{1}{n^2}\left[D_a^0\theta_a^{3.3} + HD_w^0\theta_w^{3.3}\right]$$

Figure 3 shows a series of test results on non-reactive materials (for K_r = 0), using data taken from Aubertin et al. (1999, 2000b) and Aachib et al. (2002), with D_e expressed as a function of the degree of saturation S_r. Also shown are the curves corresponding to the Collin (1987) model (equations 18-23) and to equation 24, for a (total) porosity of 0.4 (taken as an average for these test results). As can be seen, both curves provide estimated values that are in relatively good

agreement with the measured values. As mentioned above, such predictive equations provide the starting point in the iterative process to obtain D_e from testing results.

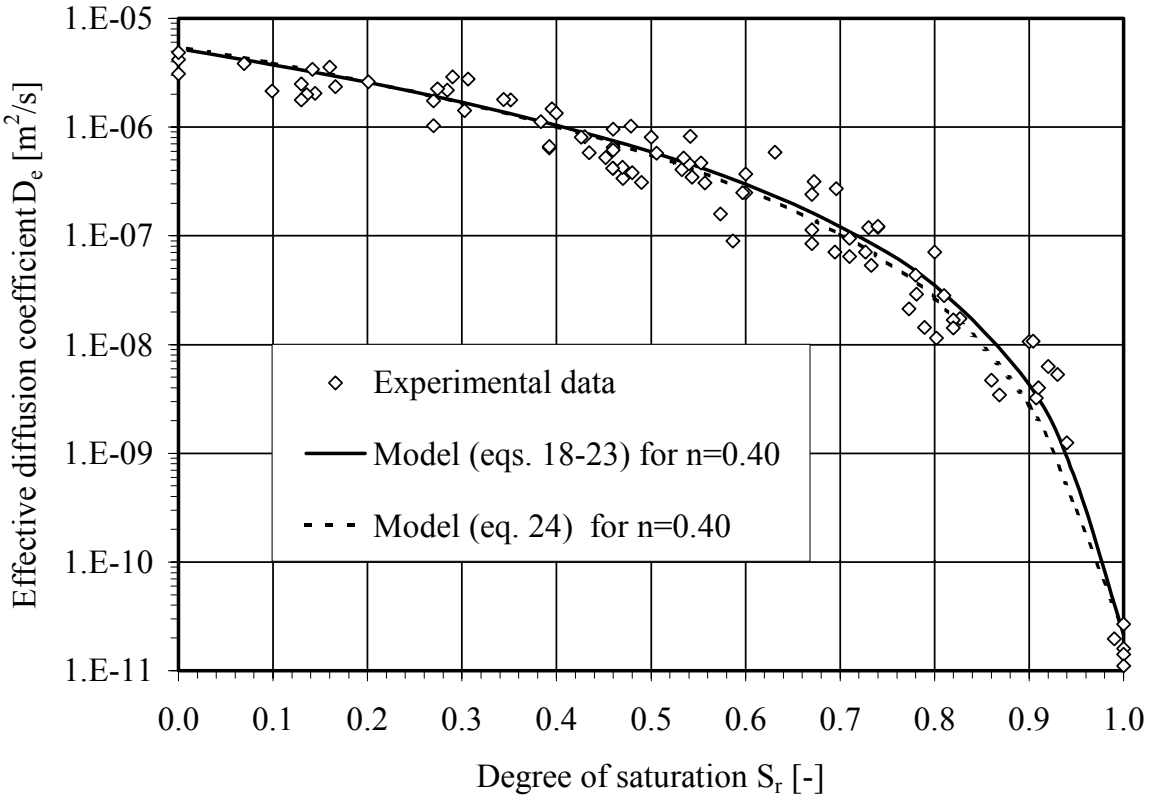

Figure 3. Comparison between diffusion coefficient values measured for different materials (soils, tailings and geosynthetic clay liners – data taken from Aubertin et al. 1999, 2000b, and Aachib et al. 2002) at various S_r, with predicted values obtained with eqs. 18-23 and eq. 24.

For the reaction rate coefficient K_r, Collin (1987, 1998) has proposed a simple model based on surface kinetic, where the rate varies linearly with the proportion of sulphide minerals (i.e. pyrite). The expression takes into account the total porosity and the grain size through an equivalent grain size diameter D_H. This equation can be written as:

$$[25] \qquad K_r = K' \frac{6}{D_H}(1-n)C_p$$

where K' is the reactivity of pyrite with oxygen ($K' \approx 5\text{x}10^{-10}\text{m}^3$ $O_2/\text{m}^2\text{pyrite/s}$ or $15.8\text{x}10^{-3}\text{m}^3$ $O_2/\text{m}^2\text{pyrite/year}$ is used here); C_p is the pyrite content over mass of dry tailings (kg/kg). The value of D_H is estimated here using a relationship with grain size curve parameters, developed for hydraulic functions (Aubertin et al. 1998; Mbonimpa et al. 2001):

$$[26] \quad D_H = [1 + 1.17 \log(C_U)] D_{10}$$

where D_{10} [L] is the diameter corresponding to 10 % passing on the cumulative grain-size distribution curve and C_U [-] is the coefficient of uniformity ($C_U = D_{60}/D_{10}$).

For a typical tailing with $D_{10} = 5\text{x}10^{-6}$ m, $C_U = 9$ and $n = 0.44$, the estimated value of K_r is around $1.59\text{x}10^{-7}$/s (or 0.0137/day, or 5/year) for C_p = 0.1%, $3.97\text{x}10^{-6}$/s (or 0.343/day, or 125/year) when C_p = 2.5%, and $1.59\text{x}10^{-5}$/s (or 1.372/day, or 500/year) for C_p = 10%. Of course, the actual values of K_r may differ from the estimated ones, as K_r also depends on a number of others factors including mineralogy and type of sulphides, temperature, oxidation state and bacterial activities (e.g. Hollings et al. 2001).

3.3 Sample results

The application of the proposed interpretation method for the laboratory tests, to determine D_e and K_r, is shown in the following using POLLUTE (Rowe et al. 1994). This software has been employed extensively over the years to analyse tests results and to evaluate the flux corresponding to various cover systems (e.g. Aubertin et al. 1995, 1997c, 1999, 2000a, 2000b; Aachib 1997; Mackay et al. 1998; Yanful et al. 1999). The equations and numerical methods used in POLLUTE have been presented by Rowe and Booker (1985, 1987). This computer program was initially developed for modeling solute transport through saturated porous media. It can be used for gas diffusion in unsaturated media when the equivalent (diffusion) porosity θ_{eq} is used in place of the total porosity n.

In the code, the reaction rate coefficient is defined from a half-time life $t_{1/2}^{*}$ (as an analogy to a radioactive decay parameter) which, in the case of a first-order reaction, can be expressed as:

[27] $$t_{1/2}^{*} = \frac{ln\,2}{K_r^{*}} = \theta_{eq}\frac{ln\,2}{K_r}$$

As illustrative examples, typical parametric calculations are performed for anticipated test results. Table 1 gives the characteristics used for 6 cases investigated. For these sample calculations, the heights of the source and receptor reservoirs are fixed at 3 cm, the height of the sand layer is 2 cm, and that of the tested materials (tailings) is 5 cm. Two values for the degree of saturation S_r are considered: 0.90 (cases 1 to 3) and 0.75 (cases 4 to 6). This range of S_r-values can be observed in practice in the capillary retention layer. The coefficient of diffusion used for modeling is estimated by equations 18 to 23, which give somewhat larger (more conservative) values than eq. 24 (see Fig. 3). For each S_r, three reactivities are considered; tailings are inert (K_r = 0/s), slightly reactive (K_r = 9.51x10^{-8}/s or 3/year), and strongly reactive (K_r =6.34x10^{-6}/s or 200/year). The properties of the sand used as the underlying coarse material are kept identical for the 6 cases.

Table 1. Material characteristics used for the parametric calculations, to illustrate the test interpretation (Figures 4 and 5).

Material	S_r [-]	n [-]	θ_a [-]	θ_{eq} [-]	D_e [m^2/s]	D^* [m^2/s]	K_r [1/s]	K_r^* [1/s]	Case
Tailings	0.90	0.44	0.044	0.056	4.59x10^{-9}	8.21x10^{-8}	0	0	Case 1
							9.51x10^{-8}	1.70x10^{-6}	Case 2
							6.34x10^{-6}	1.13x10^{-4}	Case 3
Tailings	0.75	0.44	0.110	0.120	7.71x10^{-8}	6.43x10^{-7}	0	0	Case 4
							9.51x10^{-8}	7.93x10^{-7}	Case 5
							6.34x10^{-6}	5.29x10^{-5}	Case 6
Sand	0.15	0.40	0.340	0.341	3.12x10^{-6}	9.14x10^{-6}	0	0	All cases

Figures 4 and 5 show the temporal evolution of the oxygen concentration (in %) in the source and receptor reservoirs, as obtained from calculations performed with POLLUTE. The influence of oxygen consumption on the concentration values is particularly well illustrated with these results. For non reactive materials (cases 1 and 4), an equilibrium (no gradient) state is reached after a relatively short time; this time is smaller when S_r is reduced. For slightly reactive materials (cases 2 and 5), a pseudo-steady state is approached, but oxygen consumption decreases the concentration continuously. For a large reactivity (cases 3 and 6), the influence of oxidation is very significant and equilibrium occurs only when all the available oxygen has been consumed.

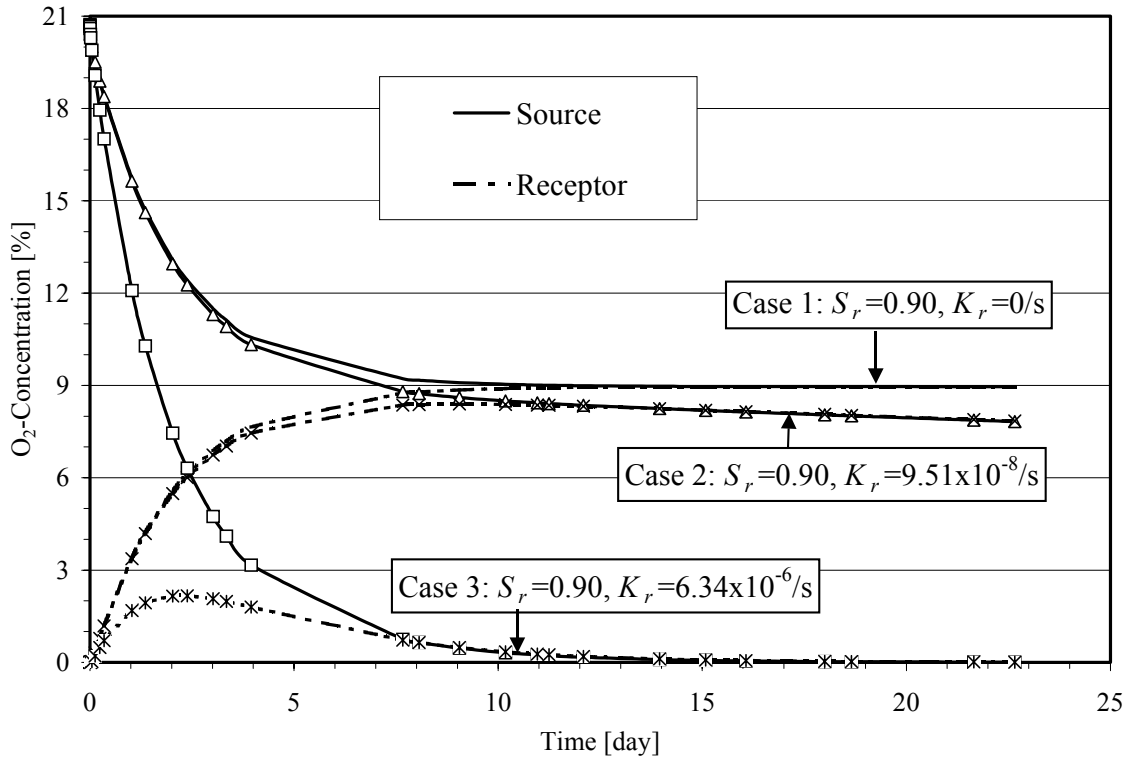

Figure 4. Temporal evolution of concentration in the source and receptor reservoirs, obtained numerically with POLLUTE, for typical testing conditions (cases 1 to 3 in Table 1).

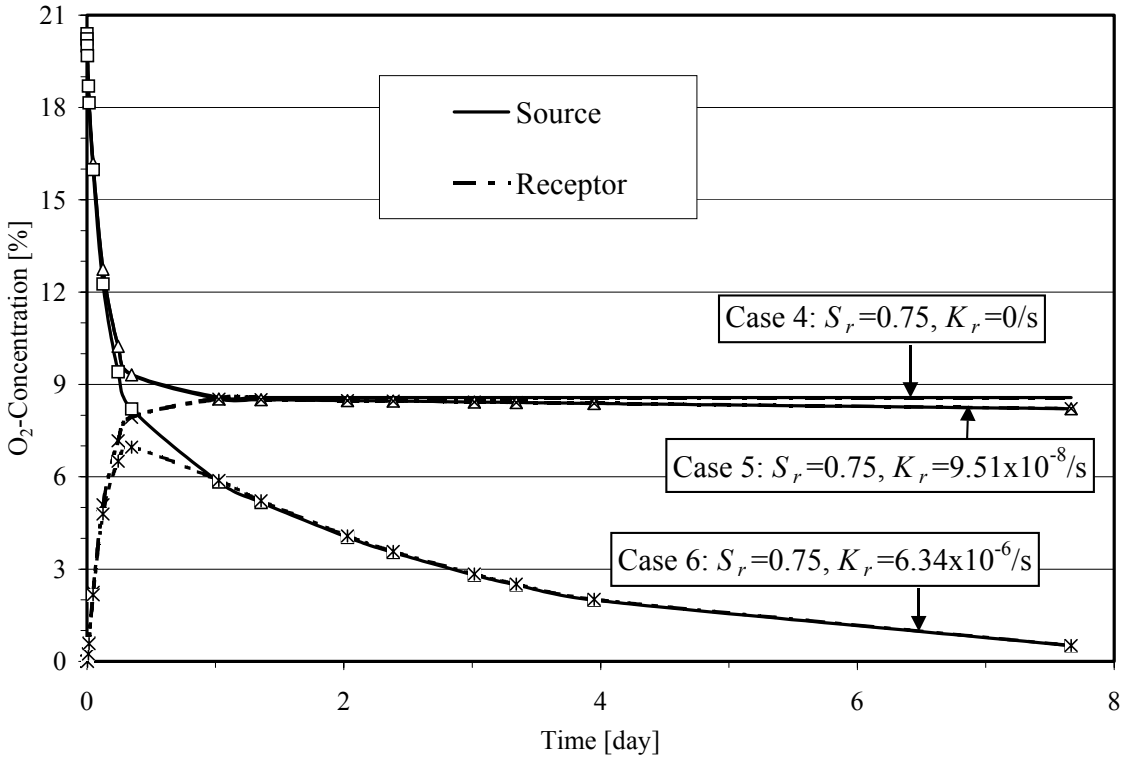

Figure 5. Temporal evolution of concentration in the source and receptor reservoirs, obtained numerically with POLLUTE, for typical testing conditions (cases 4 to 6 in Table 1).

The proposed measuring approach and corresponding interpretation were used to determine the actual oxygen diffusion coefficient D_e and reaction rate coefficient K_r of two reactive tailings (from sites SC and LTA located in Québec). The curves with the back calculated values of D_e and K_r for which concentration profile approximately match the experimental data are shown in Figures 6 and 7. In these two cases, the D_e and K_r values are fairly close to estimated values obtained from the semi-empirical solutions given above. The results show in particular that the tailings from site LTA are highly reactive (K_r=5.33x10^{-6}/s, or 168 /year). This site has been covered with a layered system.

The measurement approach presented here for laboratory tests can also be adapted to in situ conditions (e.g. Aubertin et al. 2000a; Mbonimpa et al. 2000), but this aspect is not presented here.

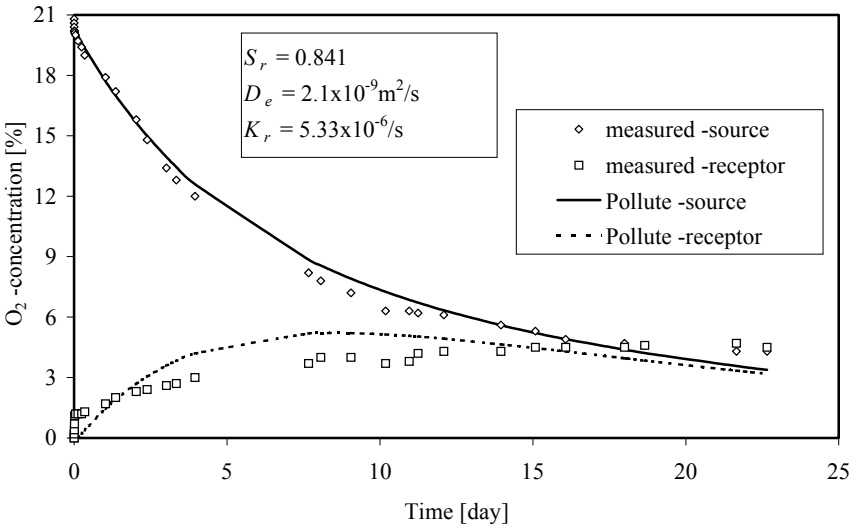

Figure 6. Estimates of D_e and K_r by comparison of the concentration values evaluated with POLLUTE and measured in lab tests on SC tailings (height of sample = 47.1 mm, height of source reservoir = 31.9 mm, height of receptor reservoir = 30.8 mm, and n=0.455).

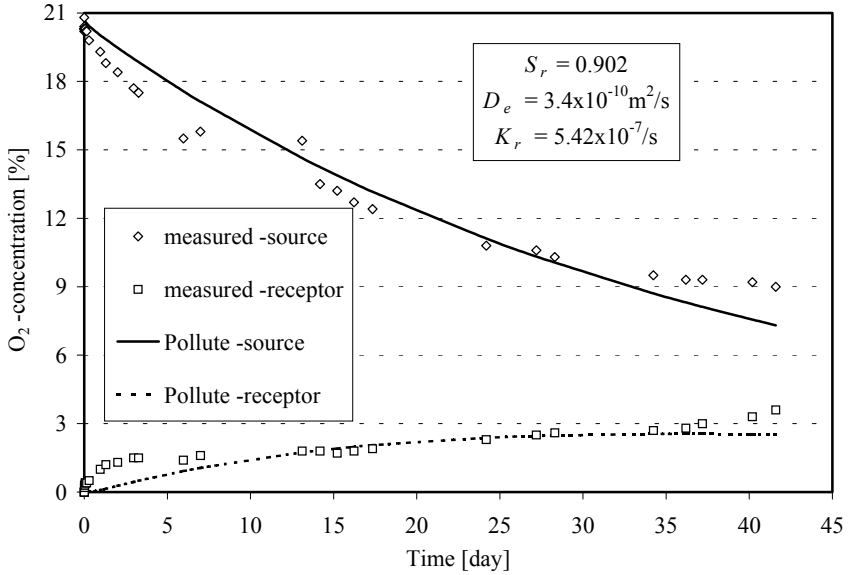

Figure 7. Estimates of D_e and K_r by comparison of the concentration values evaluated with POLLUTE and measured in lab tests on LTA tailings (height of sample = 48.2 mm, height of source reservoir = 27.8 mm, height of receptor reservoir = 30.8 mm, and n=0.480).

4. TYPICAL APPLICATIONS

4.1 Reference systems and basic calculations

The analytical equations presented above are now used to estimate the oxygen fluxes at the base and at the surface of a partly saturated, reactive or non-reactive, cover material. To validate the proposed equations, the resulting solutions are first compared to those obtained from numerical calculations. Various cases have been investigated, and some of the most relevant results are presented in the following. More emphasis is placed on the oxygen flux at the base of the cover (eq. 14) than at the cover surface (eq. 17), because the former is more relevant for the evaluation of cover efficiency.

The system being investigated here is a CCBE made of 3 layers: sand/silt/sand (layers C-D-E in Figure 1). It is similar to covers installed at the LTA site (McMullen et al. 1997; Ricard et al. 1997, 1999) and at the Lorraine site (Dagenais et al. 2001). Three cases (A, B and C) have been considered for these oxygen flux calculations. In all cases, an artificial silt (tailing) has been used for the water retention layer (see Table 2). The tailings in the cover for cases A and B are non-reactive ($K_r = 0$), while those of case C are slightly reactive (but non acid generating). It should be recalled here that such type of cover has been investigated thoroughly for unsaturated flow and water distribution using instrumented column tests (Aubertin et al. 1995, 1997c; Aachib 1997), inclined layered systems (Aubertin et al. 1997b; Bussière 1999; Bussière et al. 2000), and *in situ* experimental cells (Aubertin et al. 1997a, 1999). Field work has also been performed on an actual CCBE made with a slightly reactive tailing (Aubertin et al. 2000a).

For the calculations presented below, the values of D_e were obtained from equations 18-23, for situations representing worst case scenarios in terms of the degree of saturation (i.e. a long drought period).

Table 2. Material characteristics defined for the three-layer covers investigated (see Figures 8, 9, 10, and 23).

	Material	L (cm)	n (-)	e (-)	γ_d (g/cm^3)	S_r (%)	θ_{eq} (-)	D_e (m^2/s)	D^* (m^2/s)	$\overline{\theta}_{eq}$ (-)	$\overline{D}^*$ (m^2/s)	K_r (1/s)
A	Sand	30	0.29	0.41	2.04	13.5	0.2520	2.28E-06	9.05E-06	0.0914	5.64E-07	0
	Tailings	60	0.46	0.87	1.69	83.1	0.0890	2.42E-08	2.72E-07			
	Sand	40	0.29	0.40	2.05	28.3	0.2104	1.27E-06	6.04E-06			
B	Sand	25	0.33	0.48	2.05	8.9	0.3015	3.10E-06	1.03E-05	0.0336	5.29E-07	0
	Tailings	30	0.44	0.80	1.56	95.2	0.0338	5.34E-10	1.59E-08			
	Sand	45	0.30	0.42	2.05	24.6	0.2284	1.54E-06	6.75E-06			
C	Sand	30	0.33	0.49		5.0	0.3140	3.56E-06	1.13E-05	0.0783	4.10E-07	3 values[1]
	Tailings	80	0.44	0.80		85.0	0.0770	1.61E-08	2.09E-07			
	Sand	50	0.40	0.67		15.0	0.3418	3.12E-06	9.14E-06			

[1] Three different K_r values: 3.17×10^{-8}, 1.59×10^{-7}, and 4.76×10^{-7} per second (or 1, 5, and 15 per year respectively)

The actual boundary conditions in the field correspond fairly well to those presented above for the analytical solutions (equations 9 and 14). Above the cover and in the top sand layer (which is easily drained), the oxygen concentration $C(z=0,\ t\geq 0)$ is C_0 = 0.276 kg/m^3. Below the cover, it has been considered that concentration $C_L\ (z \geq L,\ t>0)=0$, which is a conservative (pessimistic) condition that corresponds to a rapid oxygen consumption by the reactive tailings under the cover. This condition provides the upper bound value of the concentration gradient between the top and bottom part of the cover, and thus the upper bound value of the available oxygen flux (all other factors being equal).

For the situations of interest, POLLUTE does not directly calculate the flux F at the bottom and surface of the cover (or of the water retention layer). It rather provides a concentration profile over time and the total amount Q of the substance diffusing through the cover at a given depth z and time t_a (i.e. $Q = \int_0^{t_a} F(z,t)dt$, where t_a is the active diffusion period). The flux can nevertheless be obtained by either differentiation the Q-t relation $(\delta Q/\delta t)$ or simply by using equation 1 and the concentration of two adjacent points $C(z$, and z-$\delta z)$ at time t (Aubertin et al. 1999; Joanes 1999).

For the sample calculations shown here, it is assumed that material and moisture distribution in each layer are uniform, and that parameters θ_{eq}, D_e and K_r take a constant value for the calculation period. With POLLUTE, these simplifications are not required as it is possible to work with parameters varying in space (by dividing the layer in sublayers) and over the time (by integrating for different conditions). The examples shown here nevertheless help to illustrate the calculation process, and to validate the analytical solutions.

In a 3 layer–system (sand/silt/sand), it has been demonstrated previously that during a drought, the two drained sand layers have the same O_2-concentration as the adjacent media because of their high D_e compared to the silt, hence, C_0 =0.276 kg/m^3 in the top sand layer and C_L=0 in the bottom sand layer (Aachib et al. 1993). The calculation procedure, with equations 9 and 14, can then be applied to the water retention layer only. It is shown in Figure 8, from calculations made

with POLLUTE, that neglecting the presence of the two sand layers when evaluating the oxygen flux provides essentially the same results as when incorporating them in the calculations. The limitation to this approach is further addressed below.

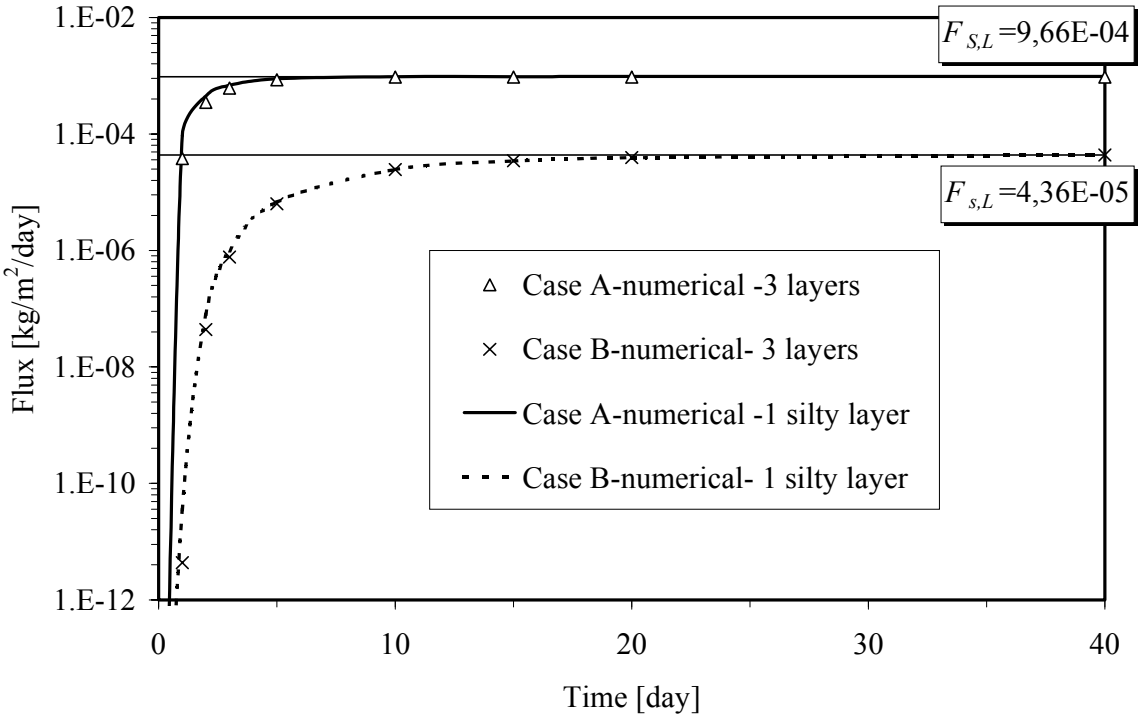

Figure 8. Comparison of temporal evolution of the oxygen bottom flux obtained by numerical solution for the three-layered systems A and B described in Table 2, and for the moisture retention (silty) layer alone; $F_{s,L}$ is the steady state flux given by eq. 10.

Figure 9 makes a comparison between the flux at the base of the cover (or the water retention layer) obtained from equation 9 and with POLLUTE, for cases A (low saturation) and B (high saturation), with a non reactive material (i.e. water retention layer). The results obtained by both approaches show an excellent agreement. In these two cases, a steady state flux is reached after about 7 days (case A) and 30 days (case B), as was predicted by equation 10. This Figure shows the influence of the cover characteristics on the flux. The total amount Q of oxygen reaching the tailings is provided by the surface below the curve for the given period. Knowing beforehand the

amount of time required to reach steady state, starting with $F = 0$ after the freezing winter months, is very important to obtain Q for the final design configuration.

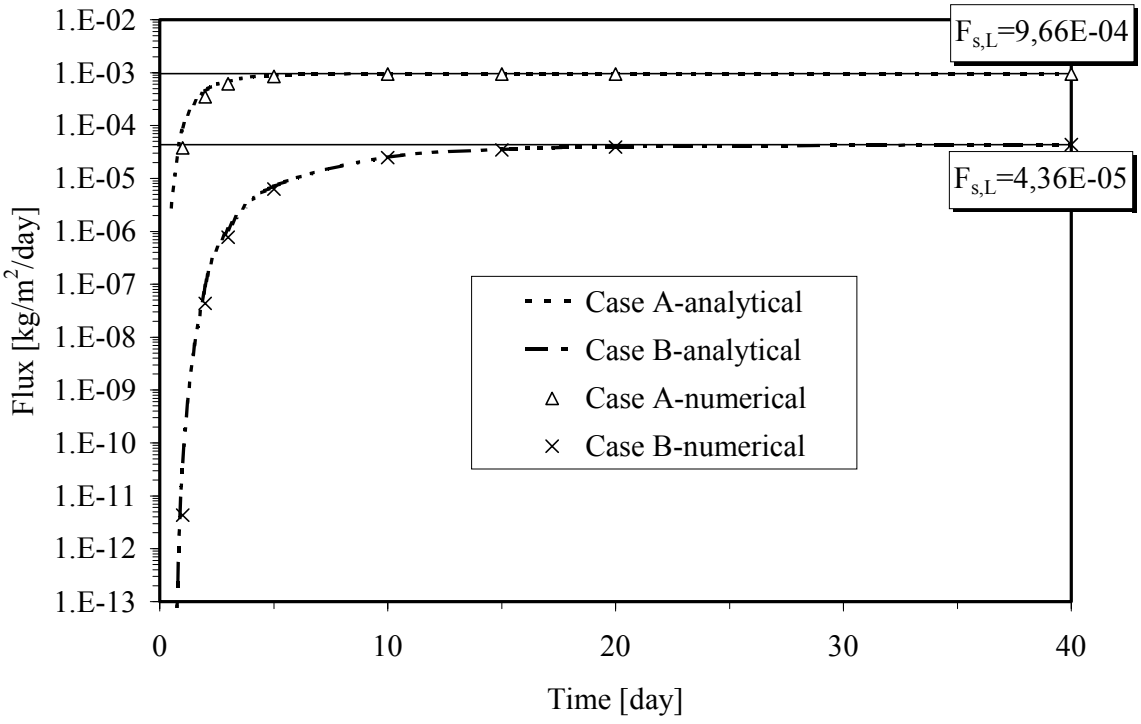

Figure 9. Comparison of the temporal evolution of the oxygen bottom flux obtained by analytical and numerical solutions on structure A and B (see Table 2) built with non reactive materials; the analytical solutions are applied to the moisture retention layer alone; $F_{s,L}$ is the steady state flux given by eq. 10

When the silt (water retaining) layer contains some small amount of reactive minerals (i.e. sulphides in tailings), it consumes part of the oxygen that diffuses through it. As stated above, this can be helpful in reducing the amount of O_2 that reaches the reactive tailings underneath. Figure 10 shows a comparison between the proposed analytical solution (equation 14) for system C (Table 2) and the solution obtained from POLLUTE. Three values of the reaction rate parameter K_r have been considered: $K_r = 3.17\text{x}10^{-8}$, $1.59\text{x}10^{-7}$, and $4.76\text{x}10^{-7}$ per second (or 1, 5, and 15 per year respectively). The oxygen flux corresponding to the non-reactive case ($K_r = 0$) is

also presented in the Figure to illustrate the effect of cover material reactivity on the flux. From Figure 10, it can be concluded that the analytical solution is in excellent agreement with the numerical solution. It also shows that increasing K_r of the cover material can significantly reduce the amount of oxygen reaching the reactive material.

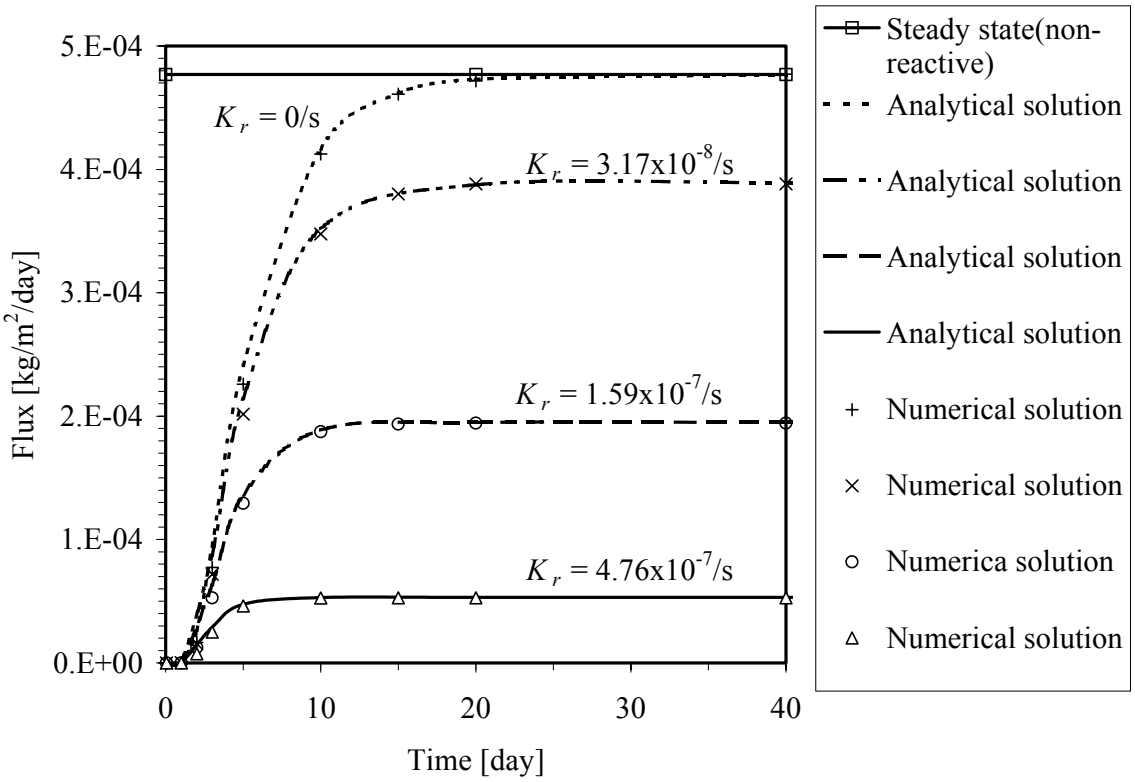

Figure 10. Temporal evolution of the oxygen flux at the base obtained by analytical and numerical solutions, in the case of a reactive moisture retention material layer for various K_r values (system C in Table 2); the analytical solutions are applied to the moisture retention layer alone.

Relatively to the temporal evolution of the surface flux entering the cover, analytical results obtained with equation 17 have also been validated with POLLUTE (results not shown here). Such surface fluxes and those reaching the base of the cover are shown in Figure 11, in the case of a water retention material layer with a thickness of 0.8 m, a porosity of 0.44, a degree of saturation of 0.85, and a diffusion coefficient estimated with equations 18–23.

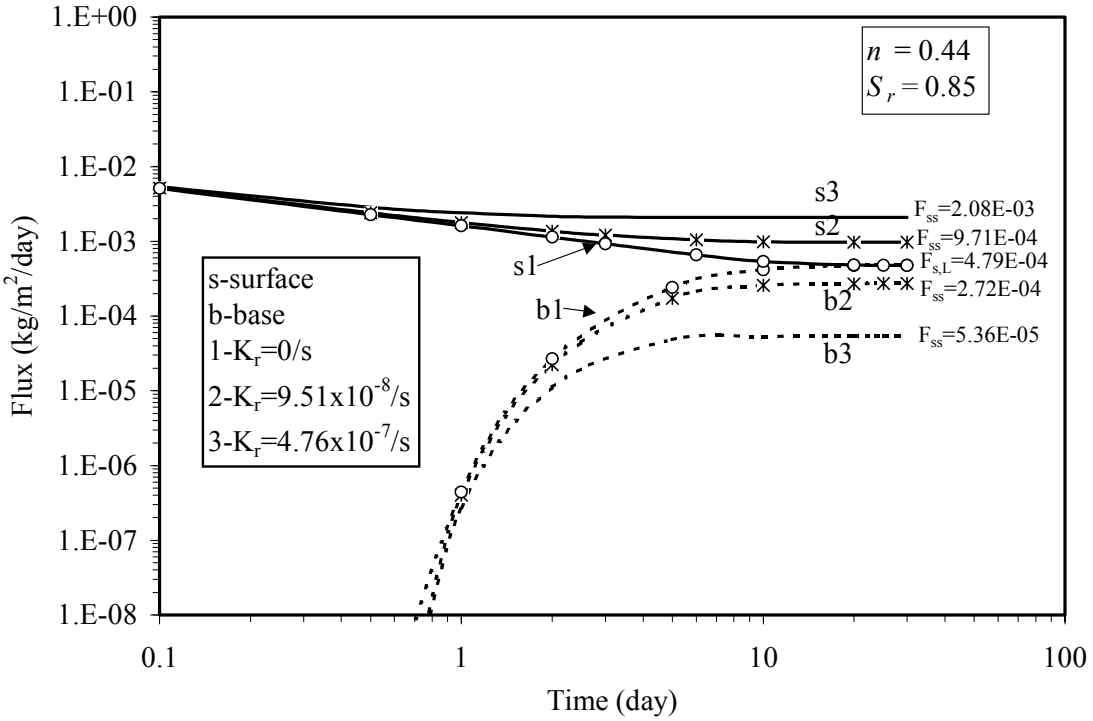

Figure 11. Temporal evolution of the base and surface fluxes obtained from analytical solutions (eqs. 14 and 16 respectively) in the case of a reactive material layer with a porosity of 0.44 and a degree of saturation of 0.85 (the diffusion coefficient is estimated with relations 18 –23), with three different reaction rate coefficients; $F_{s,L}$ and F_{ss} are the steady state fluxes (calculated with eqs. 15 and 17 respectively).

The influence of oxygen consumption is also seen from Figure 11, where three different reaction rate coefficients K_r (0, 9.51×10^{-8}, and 4.76×10^{-7}/s or 0, 3, and 15/year) have been considered. The surface flux entering the cover decreases over time while the flux reaching the base of the cover increases. These fluxes eventually reach a steady state (when the boundary conditions don't change). For reactive materials, the base and surface steady state fluxes given by equations 15 and 17 are different. The smaller the value of K_r, the smaller is the difference between the two steady state fluxes. This difference corresponds to the amount of oxygen being consumed by the cover material. In the case of a non-reactive material (K_r=0/s), the steady state flux established is obtained with equation 10; it is the same for surface and base fluxes (see curves s1 and b1 in Figure 11).

4.2 Time to reach steady state

The validity of the analytical solutions developed to evaluate the oxygen flux entering the surface and reaching the base of the cover (eqs. 14 and 16) has been confirmed using comparisons with numerical solutions provided by POLLUTE. Steady state flux equations (eq. 10, 15 and 17) were also derived from the general transient solutions, for $t \rightarrow \infty$. In the case of non reactive materials, the actual time t_{ss} necessary to reach steady state ($F_{s,L}$ given by equation 10) can be determined using the approximate expression proposed by Crank (1975) (see equation 11). Further investigations have been performed to evaluate more precisely the time necessary to attain 99.99% ($t_{ss\text{-}99.99}$), 99.0% ($t_{ss\text{-}99}$), 95.0% ($t_{ss\text{-}95}$) and 90% ($t_{ss\text{-}90}$) of the asymptotically reached steady state flux $F_{s,L}$. Various values of S_r (0.60, 0.75, 0.85, and 0.95) and of thickness L (0.4, 0.8, 1.2, and 2.0 m) for the moisture retaining layer have been considered. The diffusion coefficient D_e (and D^*) corresponding to the S_r values was estimated again with eqs. 18-23. In accordance with equation 11, linear regressions between the corresponding t_{ss} values and L^2/D^* (with a determination coefficient $R^2 = 1$) have been obtained in all cases (see Figure 12). The proportionality factor f_p calculated in this manner varies from 1 for $t_{ss\text{-}99.99}$ to 0.30 for $t_{ss\text{-}90}$. From these results, one can deduce that the proportionality factor f_p of 0.45 suggested by Crank (1975) for equation 11 corresponds to the time necessary to reach approximately 97.8 % of the steady state flux $F_{s,L}$ ($t_{ss\text{-}97.8}$). In the following, time $t_{ss\text{-}99.99}$ (with f_p=1) is adopted for defining more rigorously the onset of steady state at the base of the cover. The results shown in Figure 12 indicate that times $t_{ss\text{-}99}$, $t_{ss\text{-}95}$ and $t_{ss\text{-}90}$ represent 54, 37, and 30% of t_{ss} (=$t_{ss\text{-}99.99}$) respectively.

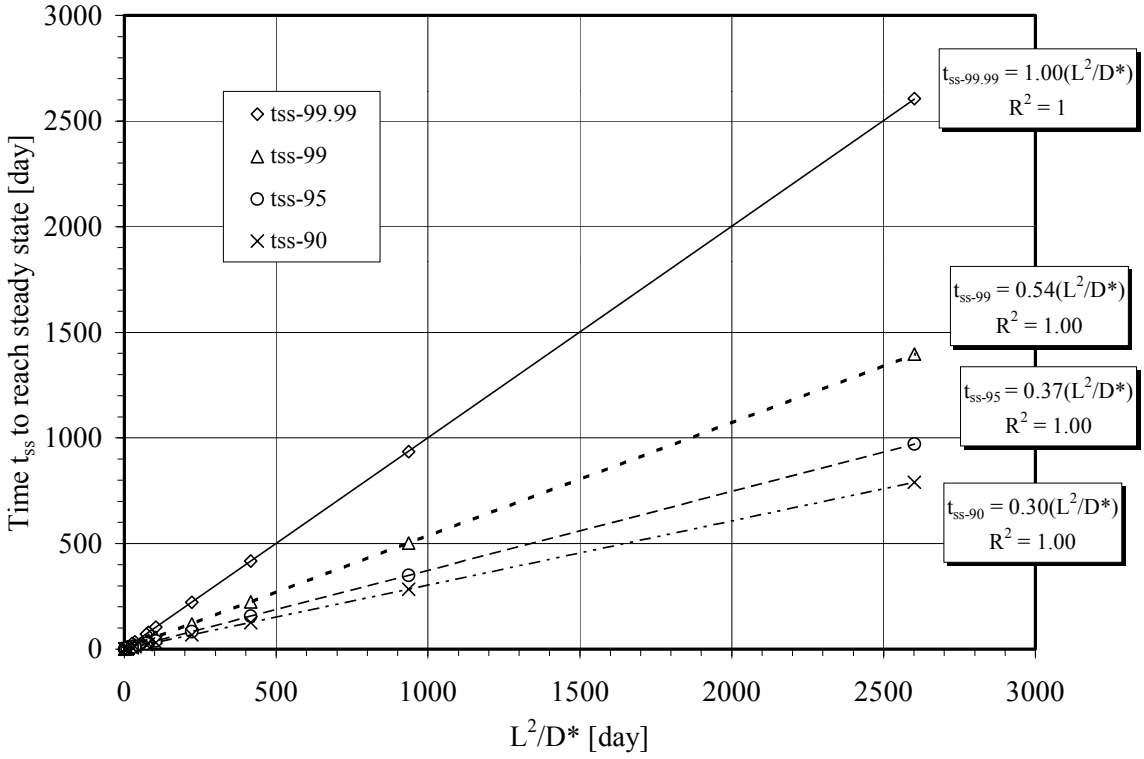

Figure 12. Time t_{ss} to reach flux values of 99.9 %, 99 %, 95% and 90% of the steady state bottom flux $F_{s,L}$ given by equation 10 for non reactive material ($K_r = 0$), for various diffusion coefficients and layer thickness; these times are respectively designated by $t_{ss\text{-}99.99}$, $t_{ss\text{-}99}$, $t_{ss\text{-}95}$, and $t_{ss\text{-}90}$.

Figure 13 shows graphically the relationship between time required to reach steady state t_{ss}, the bulk diffusion coefficient D^*, and cover thickness L. This Figure shows that in many situations corresponding to actual CCBE applications, the time required to reach steady state is not negligible compared to the duration of the available diffusion period between winter (freezing) seasons (when F=0). This means that flux calculation should typically include the transient period preceding the steady state phase, for evaluating the cover efficiency.

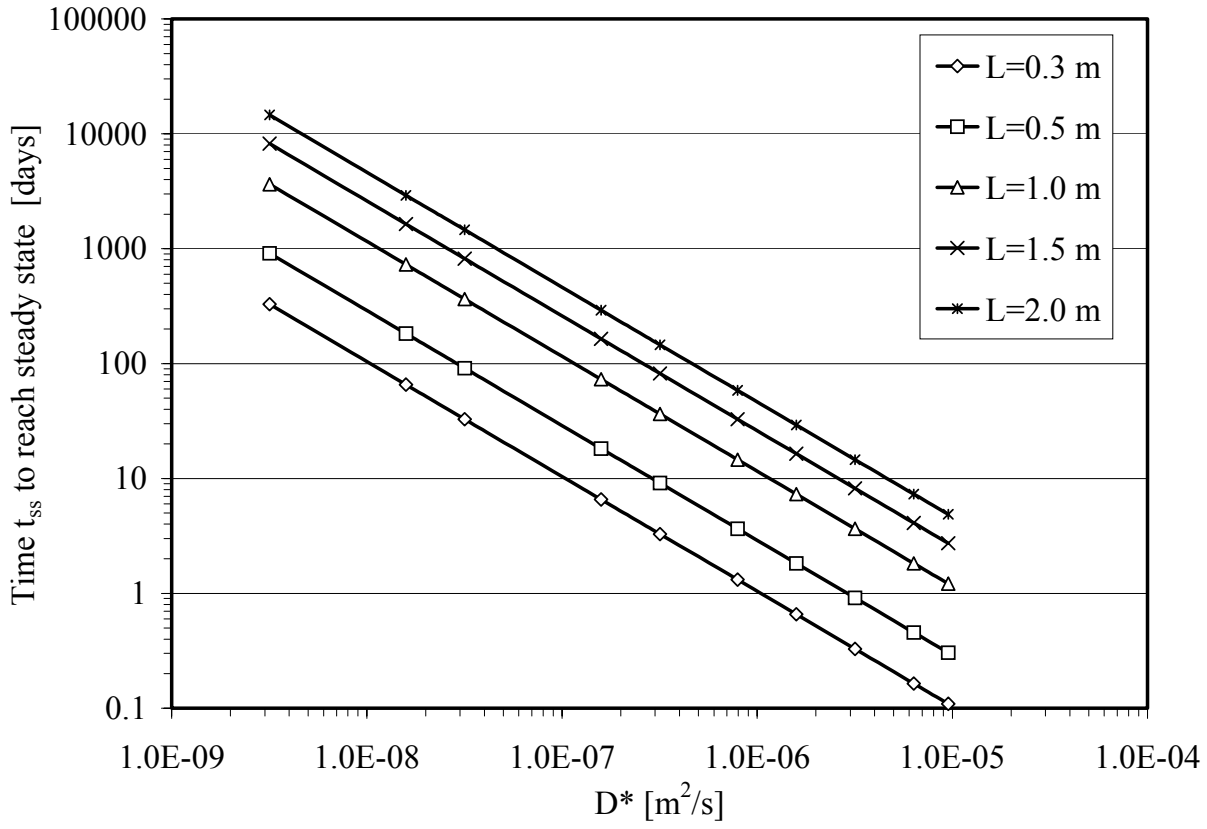

Figure 13. Estimated values of the time t_{ss} necessary to reach a steady state at the base of a cover for various diffusion coefficient D^* and layer thickness L in the case of non reactive materials using equation 11 with f_p=1.0 ($t_{ss} = t_{ss\text{-}99.99}$).

An additional investigation was performed to calculate time t_{ss} (=$t_{ss\text{-}99.99}$) at the base of the cover in the case of reactive materials for different values of S_r, L, and K_r (based on eqs. 14 and 15). Typical results are shown in Figure 14. These indicate that the time to reach steady state t_{ss} increases with the degree of saturation S_r, for given layer thickness L and oxygen consumption rate coefficient K_r. Also, t_{ss} tends to increase with L for given values of S_r and K_r, while it decreases as K_r increases for given values of S_r and L. The authors are still working to develop an appropriate analytical relationship between time t_{ss} and the influence factors D_e, L, and K_r.

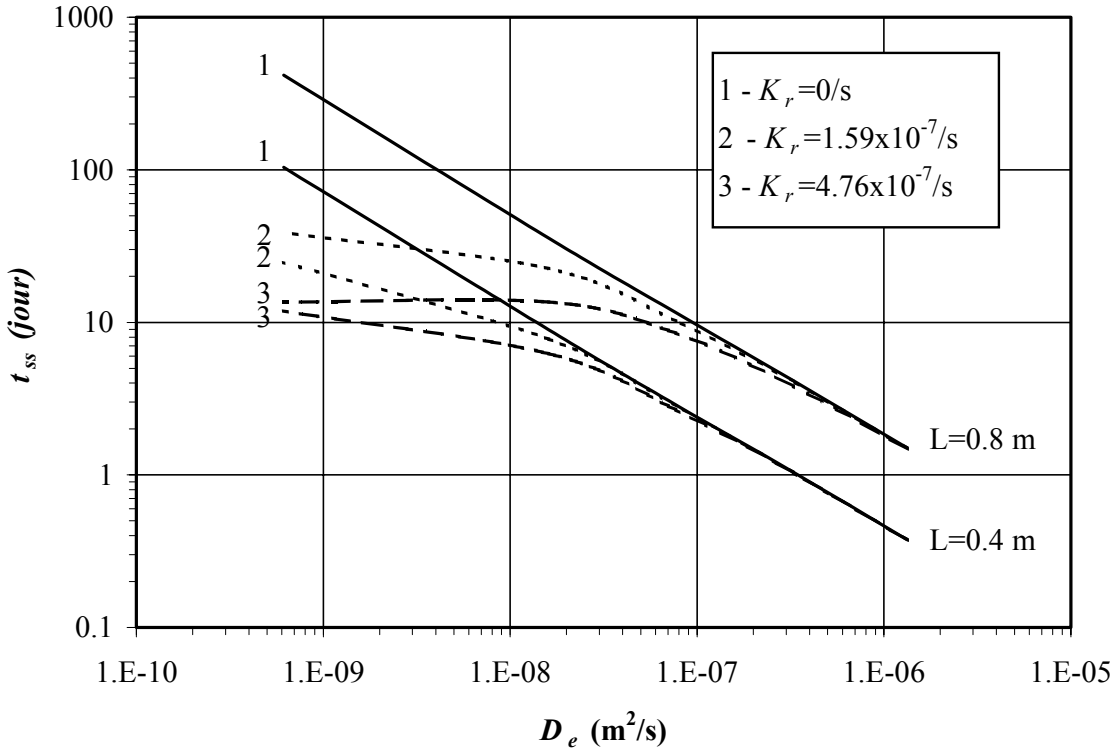

Figure 14. Time t_{ss} necessary to reach flux values of 99.9 % ($t_{ss\text{-}99.99}$) of the steady state flux given by eq. 15 at the base of reactive covers, for two thickness (0.4 and 0.8 m), various diffusion coefficients (corresponding degree of saturation between 0.40 and 0.95), and three reaction rate coefficients.

It is interesting to note also that if the flux entering the surface of the cover had been used instead to define the time to reach steady state asymptotically (see eq. 17), t_{ss} (equals here to $t_{ss\text{-}100.01}$) would be somewhat smaller than the one calculated above, except for K_r=0 when steady state is reached simultaneously above and below the cover.

4.3 Surface flux and cover efficiency

The results shown so far indicate that the expressions developed to evaluate the flux of O_2 reaching the base of a cover are well suited for parametric studies leading to decision making for cover design. With these solutions, key properties, such as degree of saturation and cover

thickness, can be varied to evaluate quickly how the cover would behave under various situations.

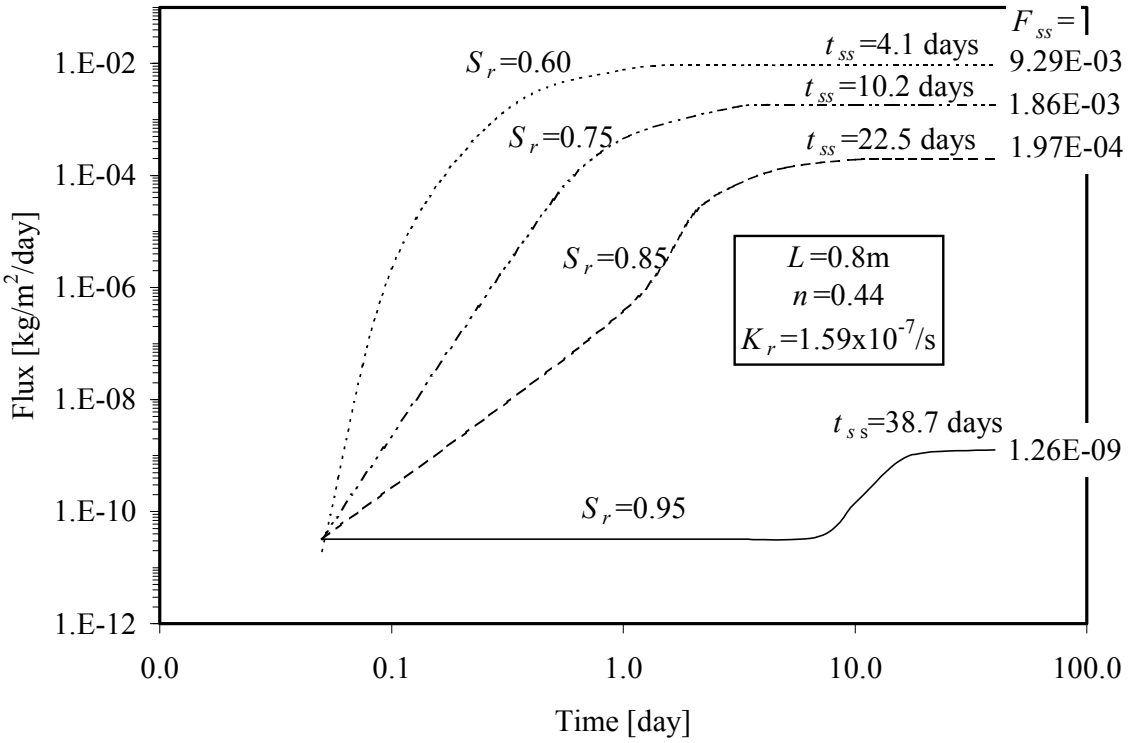

Figure 15. Influence of the degree of saturation on the evolution of the oxygen flux at the base of a cover, obtained from the analytical solution (eq. 14) in the case of a reactive material with a reaction rate coefficient K_r=1.59x10^{-7}/s, a porosity n=0.44, and a thickness L=0.8 m; the diffusion coefficient is estimated with relations 18 –23; F_{ss} is the steady state flux (eq. 15).

To further illustrate the use of these equations, the authors have drawn Figure 15 (using eq. 14) which shows how the degree of saturation (60 % ≤ S_r ≤ 95%) influences the temporal variation of the daily flux reaching the base of a cover (i.e. material layer with L=0.8m, n=0.44, and K_r=1.59x10^{-7}/s or 5/year). These plots help visualize how much the flux is being reduced when S_r is increased. These variations can range over many orders of magnitude, and influence significantly the efficiency of a cover.

One can also evaluate how S_r affects the daily flux at various times, taking into account the transient phase that precedes steady state (with eq. 14). Again, one can see on Figure 16 that the degree of saturation has a very important effect on the amount of O_2 that flows through the cover. The trend shown here is closely related to the S_r dependency of D_e, shown in Figure 3.

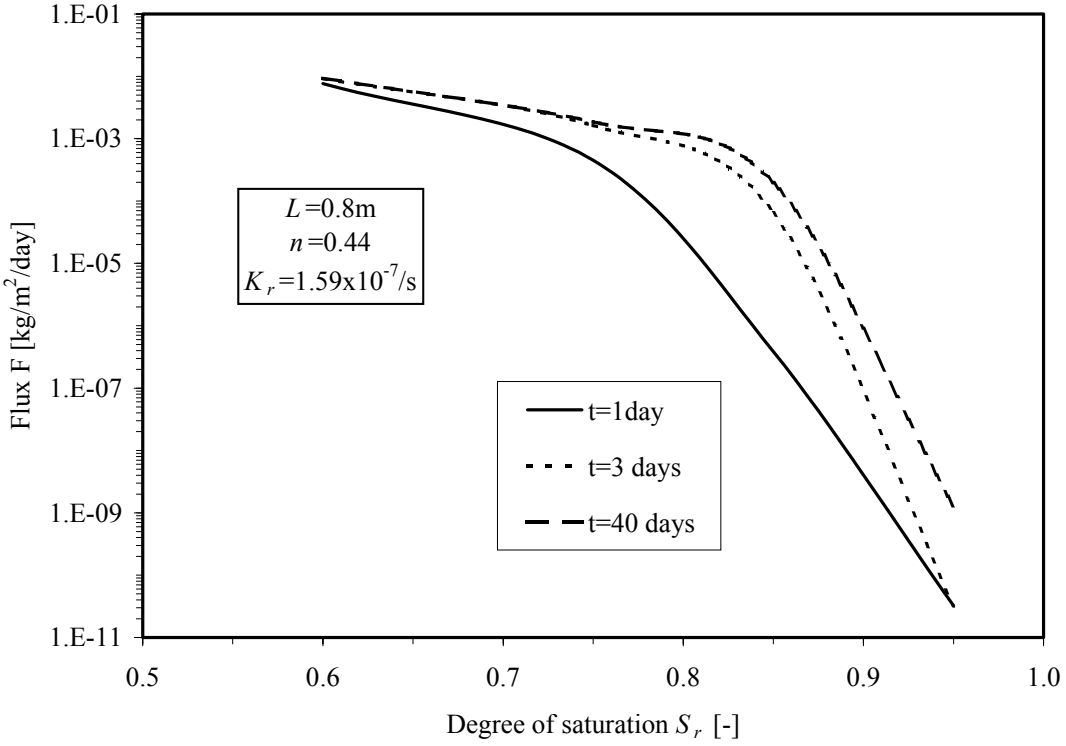

Figure 16. Influence of the degree of saturation on the oxygen flux at the base of a cover, obtained at given times from the analytical solution (eq. 14) in the case of a reactive material with a reaction rate coefficient of 1.59×10^{-7}/s, a porosity of 0.44, and a thickness of 0.8 m; the diffusion coefficient is estimated with relations 18 –23.

On the other hand, Figure 17 shows how thickness L of the moisture retention layer (with n=0.44, S_r=0.85, and K_r=1.59×10^{-7}/s) affects the transient and steady state fluxes. Increasing L reduces the daily flux and retards the onset of steady state, both beneficial factors for the cover performance.

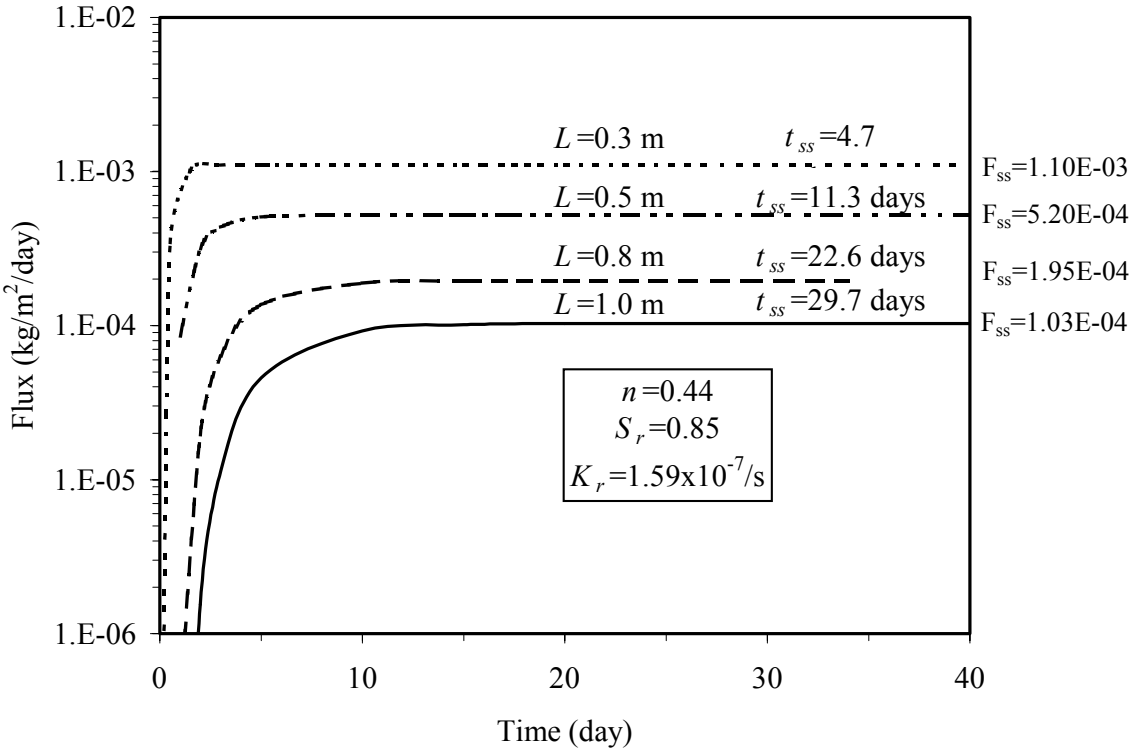

Figure 17. Influence of the water retention layer thickness L on the evolution of the oxygen flux at the base, obtained from the analytical solution (eq. 14) in the case of a reactive retention material with a reaction rate coefficient of 1.59×10^{-7}/s, a porosity of 0.44, and a degree of saturation of 0.85; the diffusion coefficient is estimated with relations 18 –23; F_{ss} is the steady state flux (eq. 15).

These solutions can be used to calculate the global amount Q of O_2 crossing through the cover. Such cumulative flux allows an evaluation of the cover efficiency by a comparison with the incoming global (daily, monthly, yearly) flux Q_o at the surface of the uncovered reactive tailings. For that purpose, the efficiency factor E is defined as follows:

[28] $$E(\%) = 100\ (1 - \frac{Q}{Q_0})$$

The smaller the value of Q, the more efficient is the cover. In this equation, the cumulative fluxes Q and Q_0 are obtained by integrating the corresponding oxygen fluxes F and F_0 over time; F is

the flux that reaches the reactive materials under the cover (given by equations 9 or 14) and F_0 is the flux at the surface of the uncovered tailings. Numerical solutions provided by the software POLLUTE can be used to estimate F_0. In this case, the tailings can be divided into sub-layers with different values of D_e and K_r (if required). Depending on the boundary conditions selected, analytical solutions can also be used to evaluate F_0 when the tailing is represented by a homogeneous layer to a depth where $C = 0$ (no more available oxygen).

4.3.1 Incoming flux for uncovered materials

The approach typically used gives an estimate of the surface flux $F_{0,s}$ under steady state conditions ($\delta C/\delta t$=0), for the following boundary conditions: $C(z=0,\ t>0)= C_0$, $C\ (z=\infty,\ t>0)= C_\infty$=0 and $C(z>0,\ t=0)$= 0 (e.g. Nicholson et al. 1989; Elberling et al. 1994; Cabral et al. 2000). The oxygen concentration profile is then given by the following specific solution of eq. 7 (for $\delta C/\delta t$=0):

[29] $$C(z) = C_0\, exp(-z\sqrt{K_r^*/D^*}) = C_0\, exp(-z\sqrt{K_r/D_e})$$

The corresponding steady state flux at different depth is obtained from equation 1 as:

[30] $$\begin{aligned} F_{0,s}(z) &= \theta_{eq} C_0 \sqrt{D^* K_r^*}\ exp(-z\sqrt{K_r^*/D^*}) \\ &= C_0 \sqrt{D_e K_r}\ exp(-z\sqrt{K_r/D_e}) \\ &= \sqrt{D_e K_r}\ C(z) \end{aligned}$$

Using eq. 30, the steady state flux entering the surface of the uncovered reactive tailings (z=0) can be evaluated as:

[31] $$\begin{aligned} F_{0,s}(z=0) &= \theta_{eq} C_0 \sqrt{D^* K_r^*} \\ &= C_0 \sqrt{D_e K_r} \end{aligned}$$

In the case of tailings with n =0.44, S_r=0.3 (leading to θ_{eq}=0.312 and D_e = 1.89x10^{-6} m^2/s) and K_r=2.54x10^{-6}/s (or 80/year), which can be considered as fairly representative values under relatively dry conditions, equation 31 leads to an oxygen flux $F_{0,s}$ = 0.052 kg/m^2/day (or 19.0 kg/m^2/year, or 594 mol/m^2/year). This calculated value however represents a lower bound of the flux for this given situation.

The boundary condition (C=0 at $z \rightarrow \infty$) adopted to obtain the solution presented above does not seem particularly realistic, especially in the case of strongly reactive tailings for which it is expected that most of the oxygen consumption occurs near the surface (e.g. Yanful 1993). It is therefore useful to determine the thickness at which the oxygen concentration in the reactive tailings becomes nil. Knowing this thickness is also required when numerical solutions are applied to evaluate the flux.

A more representative approach to evaluate the transient and steady state flux F_0 can be obtained using equations 16, when the reactive tailings are represented by an homogeneous layer with a thickness L_T satisfying the boundary conditions adopted already for developing this equation: $C(z=0, t>0) = C_0$, $C\ (z \geq L_T, t>0)$=0 and $C(z>0, t=0)$=0. Figure 18 shows the temporal evolution of the flux at the surface of uncovered tailings obtained from equation 16, for different thickness L_T (0.5, 2.0, and 8 m), with a value K_r =2.54x10^{-6}/s (or 80/year). The steady state flux F_{ss} and time t_{ss} (defined as the time necessary to reach 100.01% of the flux F_{ss}) are also given in this Figure. The porosity of the tailings is 0.44 and the degree of saturation is 0.3, leading to θ_{eq}=0.312. The effective coefficient of diffusion D_e, estimated with eqs. 18-23, is 1.89x10^{-6} m^2/s (or D^*= 6.06x10^{-6} m^2/s). Numerical calculations with POLLUTE have given identical results as these analytical solutions. It is interesting to notice here that the steady state flux of 0.052 kg/m^2/day (obtained with eq. 31) remains unchanged, in this case, for L_T greater than about 2 to 3 m. Furthermore, one sees that time t_{ss} is small (just a few days) compared to the available diffusion period. Hence, when the degree of saturation S_r is low and the reaction rate coefficient K_r is high, the transient phase can be neglected without great loss of precision. The cumulative amount of oxygen Q_0 reacting with the uncovered tailings can thus be estimated from the steady

state flux F_0. However, when tailings are highly saturated or only slightly reactive, a transient approach should be retained.

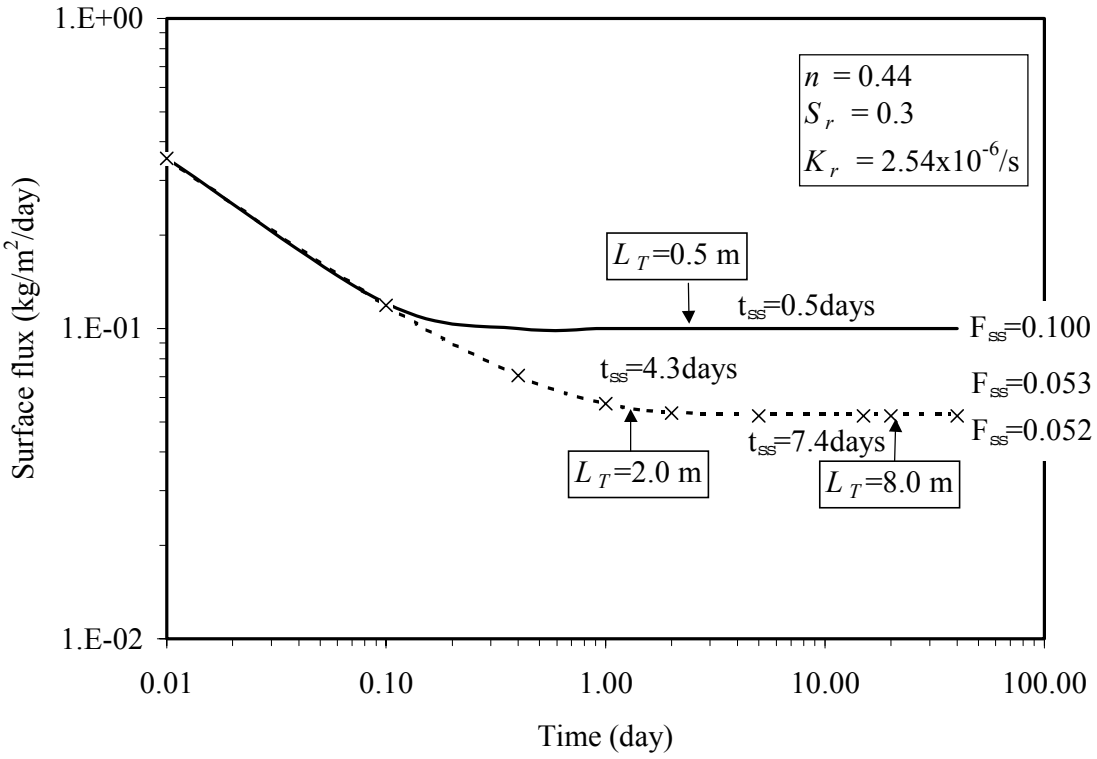

Figure 18. Evolution of the incoming surface flux F_o into uncovered tailings obtained with the analytical solution given by eq. 16, for $K_r = 2.54\text{x}10^{-6}$/s, $n = 0.44$, $S_r = 0.3$, and $L=L_T$; L_T is the depth at which the oxygen concentration is zero.

4.3.2 Reference reactive material thickness

Figure 18 also shows that the flux becomes independent of the reactive tailings thickness L_T when it exceeds a certain value, called the reference reactive tailings thickness ($L_{T,R}$). The existence of $L_{T,R}$ explains why the steady state flux obtained with eq. 31 (with $C(z=\infty, t>0)= C_\infty=0$) may be similar (or different) to the steady state flux obtained with eq. 17. In fact, $L_{T,R}$ can be defined as the value L_T making expressions 17 and 31 equivalent. For a rigorous evaluation, $L_{T,R}$ can be derived as the thickness for which $\delta F/\delta L_T=0$, where F is given by eq. 17). Because

knowing the value of this thickness $L_{T,R}$ is also required when numerical solutions are applied to evaluate the surface flux, it is useful to investigate the effect of D_e and K_r on $L_{T,R}$. For $L_T \geq L_{T,R}$, the flux calculated with eqs. 30 and 31 is independent of the tailings thickness.

Figures 19 and 20 show how the value of the reference thickness $L_{T,R}$ changes in relation with the effective diffusion coefficient D_e and the reaction rate coefficient K_r, in the case of reactive tailings with a porosity of 0.44. The results are first shown in a double-log plot of $L_{T,R}$ vs D_e (Figure 19), and then in an arithmetic plot of $L_{T,R}$ vs D_e/K_r (Figure 20).

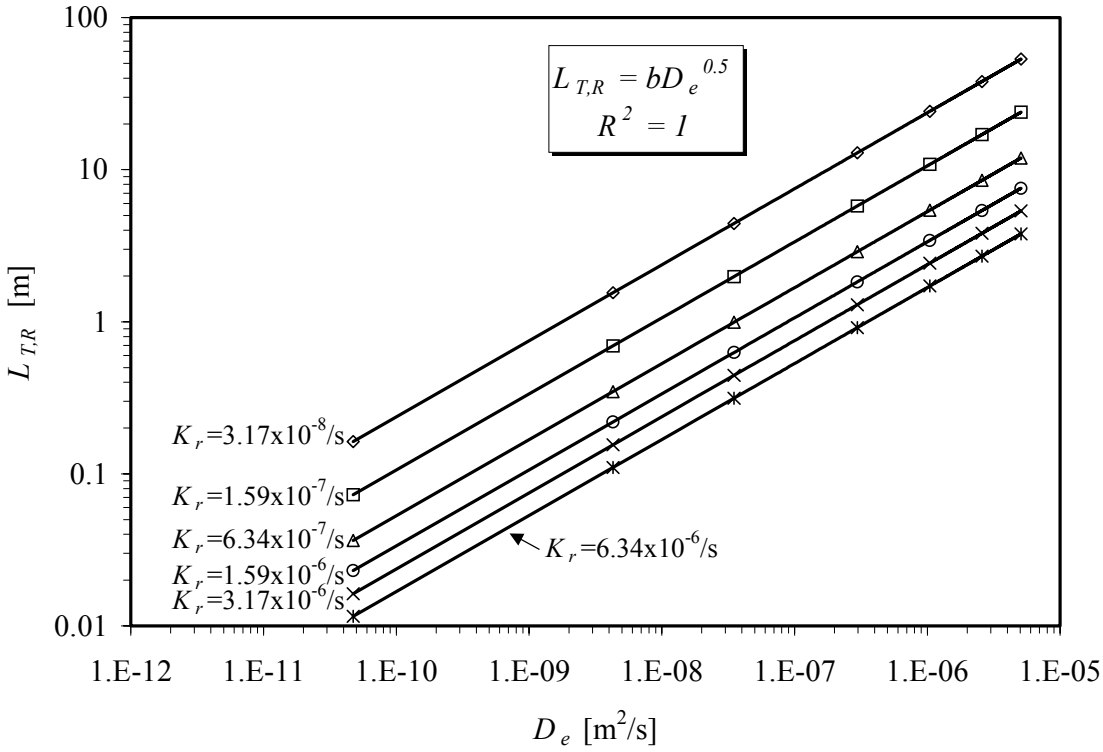

Figure 19. Effect of D_e and K_r on the reference thickness $L_{T,R}$ (for n=0.44), for which the surface flux F_0 becomes independent of the uncovered reactive tailings thickness; $b= 4.23\ (K_r)^{0.5}$

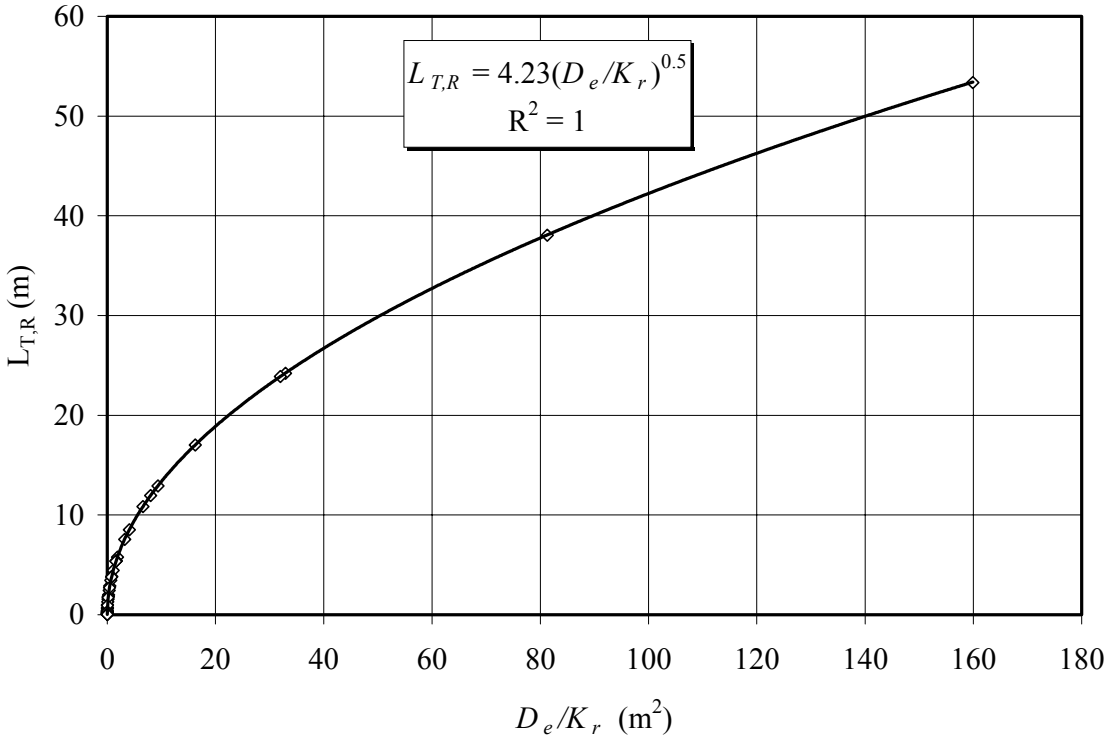

Figure 20. Relationship proposed to estimate the reference thickness $L_{T,R}$ (for n=0.44), for which the surface flux F_0 becomes independent of the uncovered reactive tailings thickness.

It can be seen that $L_{T,R}$ decreases with an increasing reaction rate coefficient K_r, and with a decreasing effective diffusion coefficient D_e (or with an increasing S_r). A simple power law equation describes the relationship between $L_{T,R}$ (m), D_e (m^2/s) and K_r (1/s):

$$[32] \qquad L_{T,R} = 4.23\left(\frac{D_e}{K_r}\right)^{0.5} = 4.23\left(\frac{D^*}{K_r^*}\right)^{0.5}$$

In equations 32, $L_{T,R}$ is expressed in m, D_e in m^2/s, and K_r in 1/s. For the case mentioned above (with n=0.44), the reference tailings thickness $L_{T,R}$ obtained with equation 32 is 3.6 m. Hence, analyses should be performed with a reactive tailings thickness of 3.6 m (or more).

4.3.3 Cumulative flux

To evaluate a cover efficiency, a comparison must be done between the consumption of O_2 with and without the cover (eq. 28). As shown previously, oxygen consumption by the moisture retention layer affects the available flux. The influence on the cumulative flux Q is shown explicitly in Figure 21 for the 3-layered system C described in Table 2.

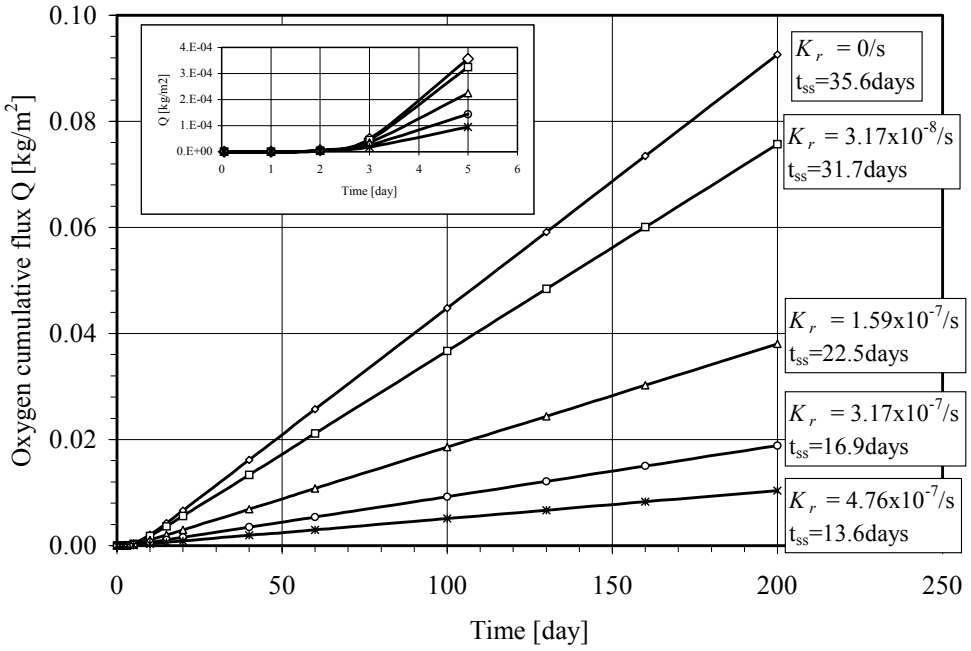

Figure 21. Influence of K_r of the moisture retaining layer material on the evolution of the cumulative flux Q that reaches the reactive tailings (with K_r= 6.34x10^{-6}/s) under the 3-layered cover (system C in Table 2); the flux Q is obtained analytically (by integrating the flux F given by eq. 14) or numerically with POLLUTE; t_{ss} is the steady state time.

Different K_r values (3.17x10^{-8}, 1.59x10^{-7}, and 4.76x10^{-7} per second, or 1, 5, and 15 per year) are assigned to the silty (water retaining) layer containing a small amount of reactive minerals. The results are furthermore compared to the non-reactive case (K_r = 0) to illustrate the influence of K_r. Because cover material can be frozen part of the year during the winter months (December to April in many parts of Canada), the oxygen flux contribution is neglected during this period. The total yearly oxygen flow is given here for an active period t_a from May to November, or 200 days

in this particular application. The temporal evolution of the cumulative fluxes Q is shown in Figure 21 for t ≤ 200 days. The same Q values were obtained analytically (by integrating the corresponding oxygen flux F given by eq. 14) and numerically with POLLUTE. It can be seen that the cumulative oxygen yearly flux Q that reaches the reactive residues under the cover decreases by a factor of about 10 for the given conditions, from 0.093 kg/m^2 for K_r = 0/s, to 0.010 kg/m^2 for K_r = 4.76x10^{-7}/s (or 15/year). Hence, as expected, consumption of oxygen can contribute significantly to the cover efficiency by reducing the amount of oxygen reaching the material underneath.

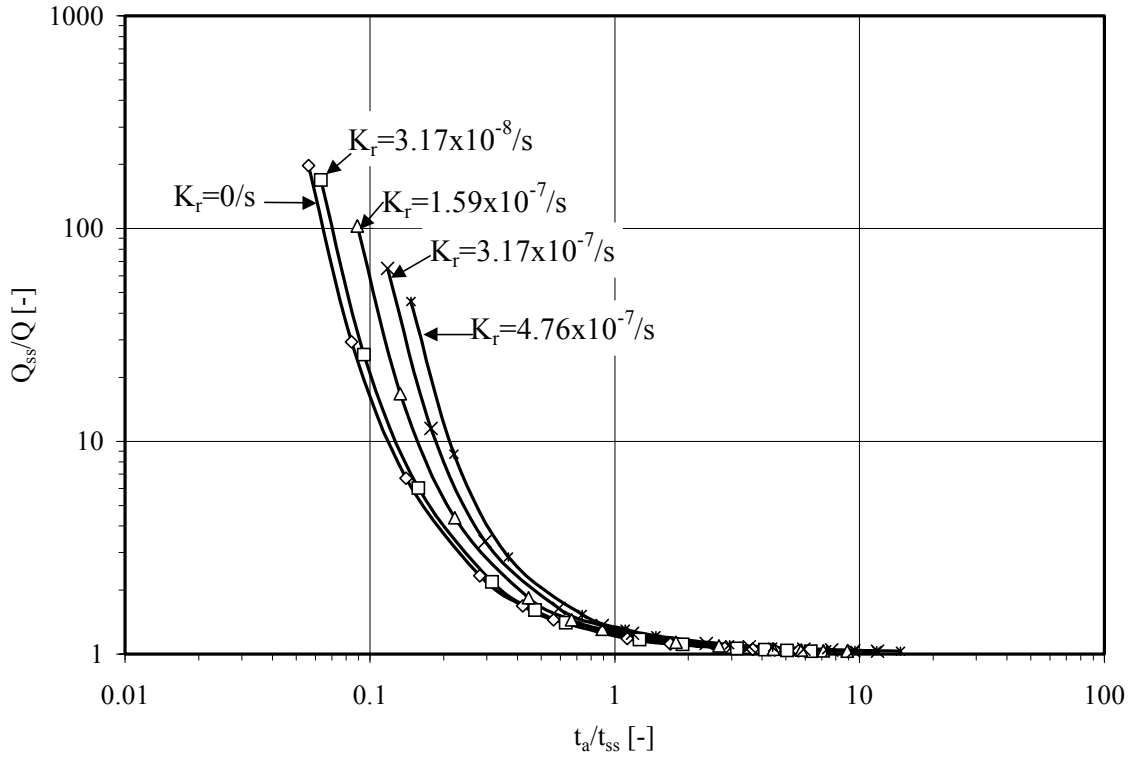

Figure 22. Influence of the active diffusion –consumption period t_a (related to the steady state time t_{ss}) on the ratio Q_{ss}/Q; Q_{ss} is the cumulative oxygen yearly flux calculated from the steady state flux F_{ss} and Q is the cumulative oxygen yearly flux calculated from the flux F including the transient phase (Q values are presented in Figure 21).

The plot presented in Figure 21, which includes the transient phase (close-up insertion), are theoretically linear for $t > t_{ss}$. Figure 22 shows the temporal variation of the ratio Q_{ss}/Q, with the

cumulative oxygen yearly flux Q_{ss} calculated from the steady state flux F_{ss} ($Q_{ss}=F_{ss}xt_{ss}$) and the total flux value Q obtained from Figure 21 (that includes the transient part of the flux). These Figures confirms that the transient flux phase for uncovered tailings is decreased when the reactivity (K_r) is increased. These results can be used to determine whether or not the transient phase should be taken into account when making the total flux evaluation.

4.3.4 Efficiency factor calculations

As a final illustration of the calculation approach, the authors have analyzed the influence of key cover properties (S_r, L and K_r) on the efficiency factor E. The application is made for a cover installed on strongly reactive tailings with n =0.44, S_r=0.3 and K_r = 6.34x10^{-6}/s (or 200/year). As the steady state time t_{ss} is small for high K_r and D_e values, only steady state flux is considered for the uncovered tailings; a steady state is assumed to exist when the cover is installed ($F_{s,0}$ = 0.083 kg/m^2/day). The amount of oxygen consumed by the uncovered tailings during a period of 200 days is 16.52 kg/m^2. Using this value as the reference cumulative flux Q_0, the efficiency factor E can now be calculated with eq. 28. Different scenarios with varying values of S_r, L and K_r for the moisture retention layer (system C, Table 2) have been treated. The influence of the oxygen consumption rate coefficient K_r for the moisture retaining material layer (with n = 0.44 and S_r = 0.85) is shown in Figure 23 for various layer thicknesses L. It can be seen that E increases non linearly with the reactivity of the cover material. To better understand the meaning of this representation, let us recall that an E value of 99.0 % corresponds to a cumulative flux Q of 0.165 kg/m^2/day, while E=99.9 corresponds to Q = 0.017 kg/m^2/day.

The effect of S_r on factor E is shown in Figure 24 for a non reactive (K_r=0) and for a slightly reactive cover material (with K_r = 3.17x10^{-7}/s or 10/year) for various layer thicknesses L. This figure shows, among other things, that increasing the value of S_r (i.e. reducing the value of D_e) is much more efficient than increasing the thickness of the cover (as previously observed by Nicholson et al. 1989). Hence, efforts should aim at improving the water retention capacity of the cover material rather than increasing the layer thickness.

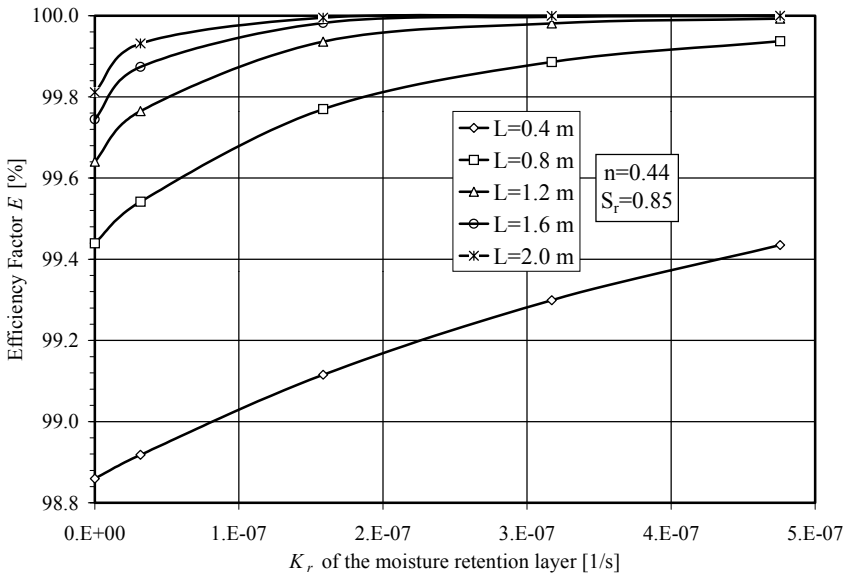

Figure 23. Influence of the oxygen reaction rate coefficient K_r of the moisture retaining material (with n=0.44, S_r=0.85, and various thickness L) on the cover efficiency factor E in the case of a cover placed on highly reactive tailings (with K_r=6.34x10^{-6}/s).

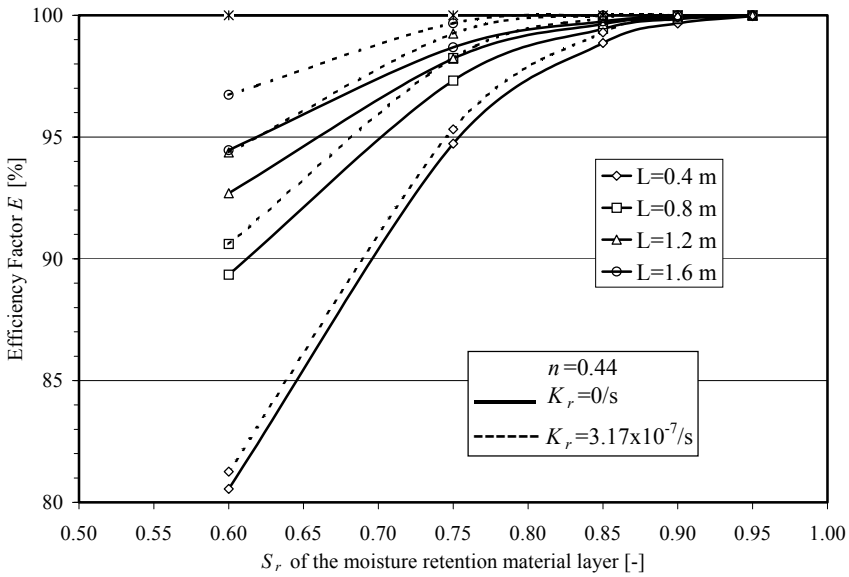

Figure 24. Influence of the degree of saturation of the moisture retaining layer on the cover efficiency factor E in the case of a cover with n=0.44, K_r =0 and K_r=3.17x10^{-7}/s placed on highly reactive tailings (with K_r = 6.34x10^{-6}/s).

5. COMPLEMENTARY REMARKS

The analytical solutions and corresponding sample calculations presented above are valid for a cover system treated as a single layer. This corresponds the case when one of the layers has a much lower D_e value than the other layers (as in many CCBE scenarios). In some situations however, it may be required to treat the cover as a true layered system to evaluate the flux, and not as a single layer. In such cases, only a numerical solution can provide (at this time) the exact solution for the transient state. The above analytical solutions can nevertheless be used for the steady state flux of non-reactive cover materials, if the diffusion coefficient is expressed as a mean weighted average for the layered system (Aubertin et al. 2000b). For that purpose, one can use:

$$[33] \qquad \overline{D}_e = \frac{\sum_{j=1}^{m} L_i}{\sum_{j=1}^{m} \frac{L_i}{D_{e,i}}}$$

or

$$[34] \qquad \overline{D}^* = \frac{\overline{D}_e}{\overline{\theta}_{eq}} = \frac{\sum_{j=1}^{m} L_j}{\sum_{j=1}^{m} \frac{L_j}{D_j^*}}$$

with

$$[35] \qquad \overline{\theta}_{eq} = \frac{\sum_{j=1}^{m} \frac{L_j}{D_j^*}}{\sum_{j=1}^{m} \frac{L_j}{\theta_{eq,j} D_j^*}}$$

In these equations, $\overline{D}_e$ and $\overline{D}^*$ are respectively the mean effective and bulk equivalent diffusion coefficients, $\overline{\theta}_{eq}$ is the mean equivalent (diffusion) porosity, m is the number of layers, and L_j,

$D_{e,j}$, and D_j* and $\theta_{eq,j}$ represent the thickness, effective and bulk diffusion coefficients, and equivalent porosity of layer j respectively.

Table 2 gives the values of $\overline{\theta}_{eq}$ and $\overline{D}^*$ calculated for cases A and B (where the single layer solution does apply well). The numerically obtained flux (with POLLUTE) for the 3 layer system, the steady-state flux (eq. 10), and the flux obtained with the analytical solution (eq. 9) using equivalent parameters (eqs. 33-35) are shown in Figure 25.

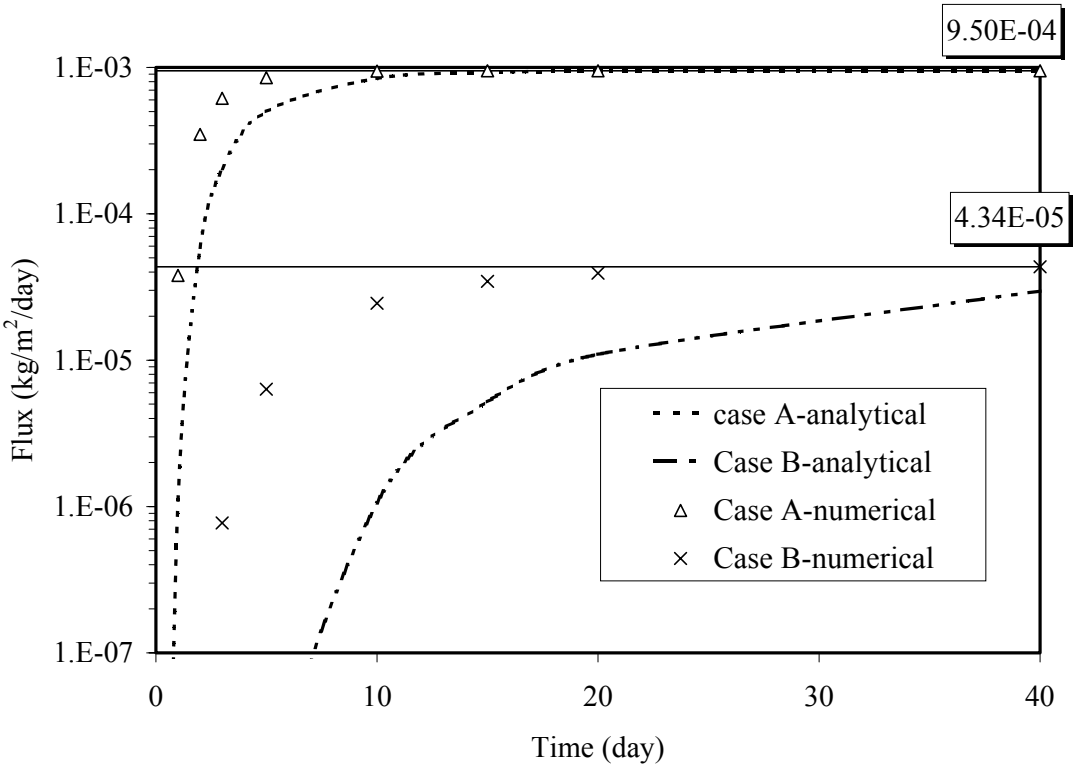

Figure 25. Comparison between the evolution of oxygen fluxes at the base obtained by the analytical solution (eq. 9) using the equivalent parameters (eqs. 33-35) and by the numerical solutions in the case of the non reactive tree-layered structure A and B (see Table 2).

As can be seen, the analytical equation does provide the correct value for steady state flux, but it fails to adequately represent the transient phase when used with these equivalent parameters. The

discrepancies between the numerical and analytical solutions are particularly important for a very effective (low flux) cover (Case B). Because the analytical solution with equivalent parameters (eqs. 33-35) tends to underestimate transient flux and overestimate t_{ss}, it is suggested not to use such equivalent parameters for transient flux calculations. They nevertheless provide a good evaluation of the steady state flux, which can be useful at the preliminary stages of a cover project.

As another note of caution on the use of analytical solutions, it is also worth mentioning here that the flux calculated from a particular solution to Fick's law presented by Crank (1975; see his equation 4.27) can sometimes be misleading. This equation has been used by the authors in the past for making preliminary calculations of oxygen flux (e.g. Aachib et al. 1994; Aubertin et al. 1999, 2000b). More recent analyses have shown however that this expression is sometimes at odd with the analytical and numerical solutions shown here, especially for the early transient phase and also for very long time periods. Thus, the authors strongly suggest that the solutions presented in this paper be used instead of the previously selected expression.

6. CONCLUSIONS

In this paper, modified Fick's laws are used to describe diffusive oxygen transport in partly saturated materials used in covers with capillary barrier effects, or CCBE. Solutions for non reactive and reactive porous materials are provided, taking into account diffusion in the air and water phases using an equivalent diffusion porosity θ_{eq}. This parameter is used with the effective diffusion coefficients D_e and the reaction (consumption) rate coefficient K_r, to write Fick's laws as functions of the bulk coefficients D^* and K_r^*, to enhance the generality of the solutions.

Analytical solutions (in form of trigonometrical series) have been proposed to calculate oxygen flux entering the surface and reaching the base of a cover system made of non-reactive (K_r=0/s) and of slightly reactive (but non acid generating) materials ($K_r \leq 4.76\text{x}10^{-7}$/s or 15/year), for transient and steady state conditions, using relatively simple but realistic boundary conditions.

The application of the proposed analytical and of existing numerical solutions requires that the oxygen flux controlling parameters for cover materials (i.e. D_e and K_r) be known in advance. For that purpose, the authors use predictive models to estimate these coefficients from basic geotechnical properties. A laboratory procedure, that allows a simultaneous determination of both parameters by measuring the flux and mass balance of O_2 in airtight cells (with a source and a receptor reservoir) is presented. Some scenarios are shown to illustrate how the oxygen concentration calculated with the code POLLUTE evolves in the two reservoirs for given materials coefficients D_e and K_r. For actual tests, an iterative back calculation process with POLLUTE provides values of D_e and K_r for which the calculated concentration profile match the experimental data. The application of this technique is shown for two reactive tailings.

The developed analytical solutions have then been applied to different scenarios considering various values of S_r (and hence of D_e), thickness L, and K_r of the moisture retaining layer. The results obtained are shown to be in very good agreement with results ensuing from a numerical treatment of modified Fick's laws.

Steady state fluxes equations have been derived from the general transient solutions. Investigations have been performed to estimate the time t_{ss} necessary to reach steady state flux at the base of a cover, for different scenarios (again varying of values of S_r, L, and K_r). For non-reactive materials (K_r =0/s), a linear relationships exists between t_{ss} and L^2/D^*. For reactive materials, the results indicate that the steady state time t_{ss} increases with S_r (for a given layer thickness L and coefficient K_r) and with L (for given values of S_r and K_r), and decreases as K_r increases (for given values of S_r and L). All others factors being equal, non reactive cover materials (K_r=0) require more time to reach the steady state.

The expressions developed to evaluate the flux of O_2 reaching the base of a cover have been used for parametric analyses showing how the cover would behave under various situations when key properties are varied. This type of analysis can be useful for decision making when designing covers. It is shown that increasing S_r and L reduces the flux and retards the onset of steady state, while increasing K_r reduces the flux but accelerates the onset of the steady state.

The authors also present some results relating the influence of cover properties to its efficiency. The efficiency factor is evaluated by comparing the amount of O_2 consumed by the tailings with and without the cover during a given active period. The surface flux reaching uncovered tailings is obtained with the analytical solution developed in the paper. The influence of reactive tailings thickness is also looked at. It is shown that the flux becomes independent of the tailings thickness L_T when it exceeds a reference thickness $L_{T,R}$. A linear expression relating $L_{T,R}$ to $(D_e/K_r)^{0.5}$ was developed. Knowing this thickness is required when numerical or analytical solutions are applied to evaluate the flux.

Finally, various analyses on the influence of key cover properties (S_r, L and K_r) on the efficiency factor E are presented. Results show that E increases with L, K_r *a*nd S_r. However, increasing the value of S_r (i.e. reducing the value of D_e) is much more efficient than increasing the thickness of the cover. The use of slightly reactive (but non acid generating) materials in the moisture retaining layer can also improve the efficiency of the cover.

7. REFERENCES

Aachib, M. 1997. Étude en laboratoire de la performance de barrières de recouvrement constituées de rejets miniers pour limiter le DMA. Ph.D Thesis, Department of Civil and Geological and Mining Engineering, École Polytechnique de Montréal, 298 pages, plus appendix (55 pages).

Aachib, M, Mbonimpa, M, and Aubertin, M. 2002. Measurement and prediction of the oxygen diffusion coefficient in partly saturated media, with applications to soil covers. Submitted for publication to Water, Air and Soil Pollution, August 2002**.**

Aachib, M., Aubertin, M., and Chapuis, R.P. 1993. Étude en laboratoire de la performance des barrières de recouvrement constituées de rejets miniers pour limiter le drainage minier acide - Un état de la question. Technical Report EPM/RT-93/32., École Polytechnique de Montréal.

Aachib, M., Aubertin, M., and Chapuis, R.P. 1994. Column test investigation of milling wastes properties used to build cover systems. Proceedings of the International Reclamation and

Mine Drainage Conference and 3rd International Conference on the Abatement of Acid Mine Drainage, Pittsburg, 2: 128-137.

Adda, Y. and Philbert, J. 1966. La diffusion dans les solides, Tome I. Presses Universitaires de Frances, Paris-VIe.

Akindunni, F.F., Gillham, R.W., and Nicholson, R.V. 1991. Numerical simulation to investigate moisture-retention characteristics in the design of oxygen limiting covers for reactive tailings. Canadian Geotechnical Journal, **28**: 446-451.

Astarita, G. 1967. Mass Transfer with Chemical Reaction. Elsevier Publishing Company.

Aubertin, M. and Chapuis, R.P. 1991. Considérations hydro-géotechniques pour l'entreposage de résidus miniers dans le nord-ouest du Québec. Proceedings of the Second International Conference on the Abatement of Acidic Drainage, Montreal, MEND/Canmet, 3: 1-22.

Aubertin, M. and Mbonimpa, M. 2001. Diffusion of oxygen through a pulp and paper residue barrier: Discussion. Canadian Geotechnical Journal, **38**: 658-660.

Aubertin, M., Ricard, J.F. and Chapuis, R.P. 1998. A predictive model for water retention curve: Application to tailings from hard-rock mines. Canadian Geotechnical Journal, 35: 55-69.

Aubertin, M., Aachib M, and Authier, K. 2000b. Evaluation of diffusive gas flux through covers with a GCL. Geotextiles and Geomebranes, **18** : 1-19.

Aubertin, M., Mbonimpa, M., and Dagenais, A.-M. 2000a. Nouvelles procédures d'essais de diffusion et de consommation d'oxygène: Applications au site LTA, Malartic, Québec. Final report submitted to Golder Associates (unpublished).

Aubertin, M., Chapuis, R.P., Bouchentouf, A., and Bussière, B. 1997b. Unsaturated flow modeling of inclined layers for the analysis of covers. Proc. 4th International Conference on Acid Rock Dranage (ICARD), Vancouver, Vol. II, pp. 731-746.

Aubertin, M., Chapuis, R.P., Bussière, B., and Aachib, M, 1993. Propriétés des résidus miniers utilisés comme matériaux de recouvrement pour limiter le DMA. Geoconfine'93, Arnould, Barrès and Cômes (eds.), Balkema, vol. I., 299-308.

Aubertin, M., Bussière, B., Aachib, M., Chapuis, R.P, and Crespo, J.R. 1996. Une modélisation numérique des écoulements non saturés dans des couvertures multicouches en sols. Hydrogéologie, **1**: 3-13.

Aubertin, M., Aachib, M., Monzon, M., Joanes, A.M., Bussière, B., and Chapuis, R.P. 1997c. Étude en laboratoire sur l'efficacité des barrières de recouvrement construites à partir de

résidus miniers. Rapport de recherche. Projet CDT 1899.3 (version préliminaire décembre 1997 – version finale mars 1999). Rapport NEDEM/MEND 2.22.2b, 110 pages.

Aubertin, M., Bussière, B., Barbera, J.-M., Chapuis, R.P., Monzon, M., and Aachib, M. 1997a. Construction and instrumentation of in situ plots to evaluate covers built with clean tailings. Proc. Fourth International Conference on Acid Rock Drainage (ICARD), Vancouver, Vol. II: 715-729.

Aubertin, M., Chapuis, R.P., Aachib, M., Bussière, B., Ricard, J.F., and Tremblay, L. 1995. Évaluation en laboratoire de barrières sèches construites à partir de résidus miniers. École Polytechnique de Montréal, NEDEM/MEND Projet 2.22.2a, 164 pages.

Aubertin, M., Bussière, B. Monzon, M., Joanes, A.-M., Gagnon, D., Barbera, J.-M., Aachib, M., Bédard, C. Chapuis, R.P., and Bernier, L. 1999. Étude sur les barrières sèches construites à partir des résidus miniers. – Phase II : Essais en place. Rapport de recherche Projet CDT P1899. Rapport NEDEM/MEND 2.22.2c, 331 pages.

Barrer, R.M. 1941. Diffusion in and through solids. Cambridge University Press, London.

Bussière, B. 1999. Étude des écoulements non-saturés à travers les couvertures avec effets de barrière capillaire. Ph.D Thesis, Department of Civil and Geological and Mining Engineering, École Polytechnique de Montréal, Québec.

Bussière, B., Aubertin, M. and Chapuis, R.P. 2000. The use of hydraulic breaks to limit desaturation of inclined capillary barriers. Proceedings of the 53rd Canadian Geotechnical Conference, Montreal, 465-472.

Cabral, A., Racine, I., Burnotte, F., and Lefebvre, G. 2000. Diffusion of oxygen through a pulp and paper residue barrier. Canadian Geotechnical Journal, **37**: 201-217.

Carslaw, H.S. and Jaeger, J.C. 1959. Conduction of Heat in Solids. Oxford University Press, London.

Collin, M. 1987. Mathematical modeling of water and oxygen transport in layered soil covers for deposits of pyritic mine tailings. Licenciate Treatise. Royal Institute of Technology. Department of Chemical Engineering. S-10044 Stockholm, Sweden.

Collin, M. 1998. The Bersbo Pilot Project. Numerical simulation of water and oxygen transport in the soil covers at mine waste deposits. Swedish Environmental Protection Agency. Report 4763, 46 pages, plus appendix.

Collin, M. and Rasmuson, A. 1988. Gas diffusivity models for unsaturated porous media. Soil Science America Journal, **52**: 1559-1565

Collin, M. and Rasmuson, A. 1990. Mathematical modeling of water and oxygen transport in layered soil covers for deposits of pyritic mine tailings. Acid Mine Drainage : Designing for closure. GAC-MAC Annual Meeting, May, 311-333.

Corey, A.T. 1957. Measurement of water and air permeability in unsaturated soil, Proceedings of the Soil Science Society of America, **21** (1): 7-10.

Crank, J. 1975. The Mathematics of Diffusion. 2nd Ed. Clarendon Press, Oxford, U.K.

Dagenais, A.-M., Aubertin, M., Bussière , B., Bernier, L., and Cyr, J. 2001. Monitoring at the Lorraine Mine Site: A follow-up on the remediation plan. 2001 National Association of Abandoned Mine Land Programs Annual Conference: Land Reborn: Tolls for the 21st Century, Athens, Ohio. Proceedings on CD-Rom.

Elberling, B., and Nicholson, R.V. 1996. Field determination of sulphide oxydation rates in mine tailings. Water Resources Research, **32** (6): 1773-1784.

Elberling, B., Nicholson, R.V., Reardon, E.J. and Tibble, P. 1994. Evaluation of sulphide oxidation rates: A laboratory study comparing oxygen fluxes and rates of oxidation product release. Canadian Geotechnical Journal, **13**: 375-383.

Freeze, R.A., and Cherry, J.A. 1979. Groundwater, Prentice-Hall, Engelwoods Cliffs, New Jersey.

Hillel, D. 1980. Fundamentals of Soils Physics. Academic Press, New York.

Hollings, P., Hendry, M.J., Nicholson, R.V., and Kirkland, R.A. 2001. Quantification of oxygen consumption and sulphate release rates for waste rock piles using kinetic cells: Cluff Lake uranium mine, northern Saskatchewan, Canada. Applied Geochemistry, 16: 1215-1230.

Jambor, J.L., and Blowes, D.W. 1994. The environmental chemistry of sulphide mine-wastes. Mineralogical Association of Canada Short Course Handbook, Vol 22, 438p.

Jin, Y. and Jury, W.A. 1996 Characterising the dependence of gas diffusion coefficient on soil properties. Soil Science society of America Journal, **60**: 66-71

Joanes, A.-M. 1999. Une analyse hydrogéochimique de l'efficacité de recouvrements multicouches pour le drainage minier acide. Applied Science Master Thesis, Department of Civil and Geological and Mining Engineering, École Polytechnique de Montréal, 208 pages

Jost, W. 1952. Diffusion in Solids, Liquids, Gases. Academic Press Inc., Publishers, New York.

MacKay, P.L., Yanful, E.K., Rowe, R.K., and Badv, K. 1998. A new apparatus for measuring oxygen diffusion and water retention in soils. Geotechnical Testing Journal, GTJODJ, **21** (4): 289-296

Marshall, T.J. 1959. The diffusion of gas in porous media. Journal of Soil Science, 10: 79-82.

Mbonimpa, M., Aubertin, M., Bussière, B. and Julien, M. 2000. Procédures et interprétation des essais de diffusion et de consommation d'oxygène en laboratoire et in situ. NEDEM 2000, Sherbrooke, Session 6, : 17-22.

Mbonimpa, M., Aubertin, M., Chapuis, R.P. and Bussière, B. 2001. Practical pedotransfer functions for estimating the saturated hydraulic conductivity. Submitted for Publication to Geotechnical and Geological Engineering.

McMullen, J., Firlotte, R., Knapp, R., and Aubertin, M. 1997. Les Terrains Aurifères Site-Site Closure and rehabilitation, conceptual to construction. In: Proceedings of the 29th Annual Meeting of the Canadian Mineral Processors Conference. Ottawa, Ontario. 21 to 23 January, pp. 273-292

MEND 2001. Mine environment neutral drainage (MEND) manual, Vol. 4: Prevention and Control, MEND 5.4.2d, Canada Centre for Mineral and Energy Technology (CANMET), Canada. 477 p.

Millington, R.J. and Quirk, J.P. 1961. Permeability of porous solids. Faraday Soc. Trans. **57**: 1200-1206.

Millington, R.J. and Shearer, R.C. 1971. Diffusion in aggregated porous media. Soil Science, **111**: 372-378

Nicholson, R.V., Gillham, R.W., Cherry, J.A., and Reardon, E.J. 1989. Reduction of acid generation in mine tailings through the use of moisture-retaining layers as oxygen barriers. Canadian Geotechnical Journal, **26**: 1-8

O'Kane, M., Wilson, G.W., and Barbour, S.L. 1998. Instrumentation and monitoring of an engineered soil cover system for mine waste rock. Canadian Geotechnical Journal, **35**: 828-846.

Reardon, E.J. and Moddle, P.M. 1985. Gas diffusion coefficient measurements on uranium mill tailings: implication to cover layer design. Uranium, **2**: 111-131.

Reible, D.D. and Shair, F.H. 1982. A technique for measurement of gaseous diffusion in porous media. Journal of Soil Science, **33**: 165-174.

Ricard, J.F., Aubertin, M., Firlotte, F.W., Knapp, R., McMullen, J and Julien, M. 1997. Design and construction of a dry cover made of tailings for the closure of Les Terrains Aurifères Site, Malartic, Québec, Canada. In : Proceedings of the 4th International Conference on Acid Rock Drainage. Vancouver, British Columbia. Vol. 4, pp. 1515-1530.

Ricard, J.F., Aubertin, M., Pelletier, P., Poirier, P., and McMullen, J. 1999. Performance of a dry cover made of tailings for the closure of Les Terrains Aurifères site, Malartic, Québec, Canada. Proceedings Sudbury'99 Mine and Environment II pp. 155-164.

Rolston, D.E., Glauz, R.D., Grundmann, G.L., and Louie, D.T. 1991. Evaluation of an in situ method for measurement of gas diffusivity in surface soils. Soil Science Society of America Journal, **55**: 1536-1542.

Rowe, R.K., and Booker, J.R. 1985. 1-D polluant migration in soils of finite depth. Journal of Geotechnical Engineering, ASCE, 11(GT4): 13-42.

Rowe, R.K., and Booker, J.R. 1987. An efficient analysis of polluant migration through soil. In Numerical methods for transient and coupled systems. Eds Lewis, Hinton, Bettess and Schrefler. John Wiley & Sons, pp. 13-42

Rowe, R.K., Booker, J.R., and Fraser, M.J. 1994. POLLUTEv6 and POLLUTE-GUI User's Guide. GAEA Environmental Engineering Ltd., London, 305p.

Scharer, J.M., Annable, W.K., and Nicholson, R.V. 1993. WATAIL 1.0 User's Manual, Institute for Groundwater Research, University of Waterloo, Canada.

Shackelford, C.D. 1991. Laboratory diffusion testing for waste disposal. A review. Journal of Contaminant Hydrology, **7**: 117-120.

Shelp, M.L. and Yanful, E.K. 2000. Oxygen diffusion coefficient of soils at high degrees of saturation. Geotechnical Testing Journal, GTJODJ, **23** (1): 36-44.

SRK 1989. Draft Acid Mine Drainage Technical Guide. BC AMD Task Force, Vol. 1.

Tremblay, L. 1995. Étude du transport de l'oxygène dans des matériaux poreux partiellement saturés. Applied Science Master Thesis, Department of Civil and Geological and Mining Engineering, École Polytechnique de Montréal, Québec.

Troeh, F.R., Jabro, J.D., and Kirkham, D. 1982. Gaseous diffusion equations for porous materials. Geoderma, **27**: 239-253.

Wilson, G.W., Newman, L., Barbour, S.L., O'Kane, M., and Swanson, D.A. 1997. The cover research program at Equity Silver Mine Ltd. In: Proccedings of the 4th International

Confernce on Acid Rock Drainage. Vancouver, British Columbia. 31 May to 6 June. Vol. 1, pp. 197-210.

Woyshner, M.R. and Yanful, E.K. 1995. Modelling and field measurements of water percolation through an experimental soil cover on mine tailings. Canadian Geotechnical Journal, **32**(4): 601-609

Yanful, E.K. 1993. Oxygen diffusion through soil covers on sulphidic mine tailings. Journal of Geotechnical Engineering, ASCE, **119** (8): 1207-1228.

Yanful, E.K., Simms, P.H., and Payant, S.C. 1999. Soil covers for controlling acid generation in mine tailings: a laboratory evaluation of the physics and geochemistry. Water, Air, and Soil Pollution, **114**: 347-375.

Zhan, G., Aubertin, M., Mayer, A., Burke, K. and McMuller, J. 2001. Capillary cover design for leach pad closure, 2001 SME Annual Meeting, Feb. 26-26, Denver, Colorado, Preprint 01-137.

L'École Polytechnique se spécialise dans la formation d'ingénieurs et la recherche en ingénierie depuis 1873

École Polytechnique de Montréal

École affiliée à l'Université de Montréal

Campus de l'Université de Montréal
C.P. 6079, succ. Centre-ville
Montréal (Québec)
Canada H3C 3A7

www.polymtl.ca

ÉCOLE
POLYTECHNIQUE
MONTRÉAL